INVESTIGATION OF THE *IN VITRO* EFFECT OF A MULTIFUNCTIONAL POLYMERIC DRUG DELIVERY PLATFORM

by

BERİL ÜSTÜNKAYA

Submitted to the Graduate School of Engineering and Natural Sciences

in partial fulfillment of

the requirements for the degree of Master of Science

Sabancı University

July 2023

..

ABSTRACT

INVESTIGATION OF THE *IN VITRO* EFFECT OF A MULTIFUNCTIONAL POLYMERIC DRUG DELIVERY PLATFORM

BERİL ÜSTÜNKAYA

Materials Science and Nano Engineering, Master of Science Thesis, 2023

Thesis Supervisor: Prof. Dr. Gözde Özaydın İnce

Keywords: Drug delivery system (DDS), Near Infrared (NIR)-responsive structures, Phototherapy, Breast cancer

The field of nanomedicine emerges a variety of approaches to fight against different types of cancer. Implantable DDSs being one of these approaches, they have been widely investigated due to their advantages of providing therapeutics directly to the site of disease and hence increased treatment efficiency. In this thesis, the *in vitro* effect of a nanofiber-based implantable DDS that was previously designed by using breast cancer as model disease was investigated. With this implantable DDS, it is aimed to completely remove the cancer cells remaining after the surgery by using phototherapy and to activate the immune system through the released proteins from the patches. First, the patch cytotoxicity, and its success in activation of the immune response was evaluated. Then, the cytotoxicity, cellular uptake, and *in vitro* phototherapeutic effect of the NIR-responsive nanostructure were evaluated upon light irradiation. The results demonstrated that the proteins successfully activated the immune system, and the NIR-responsive nanostructure was uptake by the cells with high efficiency and could demonstrate phototherapeutic effect on the targeted cells. Therefore, this DDS combining the NIR-responsive nanostructures and protein-incorporated implantable patch might be a promising alternative as it provides a good *in vitro* performance for the treatment of breast cancer.

ÖZET

ÇOK İŞLEVLİ POLİMERİK İLAÇ TAŞIMA SİSTEMİNİN *İN VİTRO* ETKİSİNİN İNCELENMESİ

BERİL ÜSTÜNKAYA

Malzeme Bilimi ve Nano Mühendislik, Yüksek Lisans Tezi, 2023

Tez Danışmanı: Prof. Dr. Gözde Özaydın İnce

Anahtar Kelimeler: İlaç taşıma sistemi, Yakın kızılötesi ışığa duyarlı yapılar, Fototerapi, Meme kanseri

Nanotıp alanı, kanserin farklı türleri ile savaşmak için yeni tedavi yöntemleri sunmaktadır. İmplant edilebilen ilaç taşıma sistemleri bu stratejilerden birisi olup, terapötikleri hastalık bölgesine direkt verme ve dolayısıyla daha etkili bir tedavi avantajı sunmaktadırlar. Bu tezde, meme kanseri model olarak kullanılarak daha önceden üretilmiş olan nanofiber temelli implant edilebilen bir ilaç taşıma sisteminin *in vitro* etkisi incelenmiştir. Bu implant edilebilen ilaç taşıma sistemi ile, ameliyat sonrasında kalan kanser hücrelerini fototerapi yöntemi ile tamamen yok etmek ve bağışıklık sistemini uyaracak antijenler ile bağışıklık sistemini aktive etmek hedeflenmiştir. İlk olarak, protein yüklü nanofiber yamanın toksisitesi, ve bağışıklık sistemini aktive etmekteki başarısı değerlendirilmiştir. Sonrasında, yakın kızılötesi ışığa duyarlı nanopartiküllerin toksisitesi, hücresel alımı ve *in vitro* fototerapötik etkileri değerlendirilmiştir. Yamadan salınan proteinlerin bağışıklık sistemini aktive etmekte başarılı olduğu; yakın kızılötesi ışığa duyarlılığı olan nanopartiküllerin yüksek verimle hücresel alımının yapıldığı ve hücreler üzerinde terapötik etki gösterebildiği gözlemlenmiştir. Sonuç olarak, yakın kızılötesi ışığa duyarlı nanopartiküller ve protein içeren implant edilebilen bu yama dizaynı meme kanserinde başarılı *in vitro* etki gösterdiği için umut vadedici bir alternatif olabilir.

ACKNOWLEDGMENTS

I would like to thank my advisor Prof. Gözde Özaydın İnce for providing me with all the opportunities and for her constant support throughout my master studies. I would like to thank my thesis committee members Assoc. Prof. Özlem Kutlu and Prof. Mehmet Burçin Ünlü for allocating their time to evaluate my thesis and giving valuable feedback. I also want to thank Assoc. Prof. Özlem Kutlu for her constant support during my studies.

This research was financially supported by TÜBİTAK with a grant number 120Z943. I thank TÜBİTAK for supporting my research.

I would like to thank Eric Meng Meng Tan, Çağrı Şenel, Cihangir Erdoğan, and Seydi Yavaş for their support in laser-related experiments.

I am grateful to Buğra Şenel for being there and helping me in the lab during one of the toughest time periods, and to Hale Kesim for teaching me the cell culture techniques. I also thank Saliha Durak for western blot assay; to Pelin Kemikli, Eyşan Mutlu, Alp Yetişgin and Gizem Çelebi for their support during my studies. I also would like to thank my project mates Eda Güney and Jalal Karimzadehkoei for all their support especially for the production of the particles and the patches. I also want to thank the members of İNCE group Faruk Can, Can Egil, Tuğçe Akkaş Mohammadmoradi for all their support.

During my time here, I made great friends whom I shared both the good and the hard times. I would like to express my gratitude to my dear Belkıs Güneş, Melis Porsuk, Gülşah Yıldız, Hale Kesim, Gizem Beliktay, Şevin Adıgüzel, Jalal Karimzadehkoei, Aybüke Özer, and Elif Kıvrak for their friendship.

I also want to express my gratitude to my dear Ezgi Uzun for being by my side all the time, and to my beloved Erdal Yankı Narin, for his endless encouragement, patience, and love.

My deepest gratitude to my mother Berrin, my father Ender, and my sister Beren who are always by my side with their unconditional love and support… I am especially grateful to have such a great sister and feel so lucky to have her guidance in my life.

TABLE OF CONTENTS

ABSTRACT iii
ÖZET iv
ACKNOWLEDGMENTS v
LIST OF SYMBOLS AND ABBREVIATIONS x
CHAPTER 1: INTRODUCTION 1
1.1. Breast Cancer and Current Treatment Methods 1
1.2. Localized Treatment for Breast Cancer 2
1.3. Aim of the Study 4
CHAPTER 2: INVESTIGATION OF THE *IN VITRO* EFFECT OF HER2 AND IGF-IR INCORPORATED IMPLANTABLE PATCHES 5
2.1. Introduction 5
2.1.1. Implantable DDSs 5
2.1.2. The Relationship of Breast Cancer with HER2 and IGF-IR 6
2.1.3. Activation of Adaptive Immune System 7
2.1.4. Aim of the study 8
2.2. Materials and Methods 8
2.2.1. Materials 8
2.2.2. Methods 9
2.3. Results and Discussion 10
2.3.1. Investigation of Patch Cytotoxicity 10
2.3.2. Investigation of HER2 and IGF-IR Loading of BDCM Cells 13
2.3.3. Assessment of Immune System Activation 15
2.4. Conclusion 16
CHAPTER 3: INVESTIGATION OF THE *IN VITRO* EFFECT OF NIR-RESPONSIVE NANOSTRUCTURE 18
3.1. Introduction 18
3.1.1. Photothermal Effect and PTT 18
3.1.2. Aim of the study 20

3.2. Materials and Methods 21
3.2.1. Materials 21
3.2.2. Methods 22
3.3. Results and Discussion 23
3.3.1. Dark Toxicity of Est/PD/RB-BT 23
3.3.2. Cellular Uptake 25
3.3.3. Investigation of Photothermal Effect *In Vitro* 27
3.4. Conclusion 28
CHAPTER 4: INVESTIGATION OF THE *IN VITRO* PHOTODYNAMIC EFFECT OF NIR-RESPONSIVE NANOSTRUCTURE 29
4.1. Introduction 29
4.1.1. Photodynamic Effect and PDT 29
4.1.2. Rose Bengal 30
4.1.3. Barium Titanate 31
4.1.4. Aim of the study 32
4.2. Materials and Methods 33
4.2.1. Materials 33
4.2.2. Methods 33
4.2.1. Investigation of *In Vitro* Photodynamic Effect of RB-BT Nanoparticles 33
4.2.2. Investigation of *In Vitro* Photodynamic Effect of Est/PD/RB-BT Nanoparticles 34
4.3. Results and Discussion 34
4.3.1. Investigation of *In Vitro* Photodynamic Effect of RB-BT Nanoparticles 34
4.3.2. Investigation of *In Vitro* Photodynamic Effect of Est/PD/RB-BT Nanoparticles 35
4.4. Conclusion 36
CHAPTER 5: CONCLUSION 38
BIBLIOGRAPHY 40

LIST OF FIGURES

Figure 1 Current treatment methods for breast cancer.....2
Figure 2 Representation of DDS.....4
Figure 3 Schematic representation of the immune system (Lowell, 2020) 7
Figure 4 The change in cell viability across experimental groups at different time points. Bars indicate SD and statistical significance was indicated with an asterisk (*p ≤ 0.05, **p ≤0.01, ***p ≤ 0.001).....11
Figure 5 : The cytotoxicity of HER2 and IGF-IR incorporated uncoated, and poly (DMAEMA-co-EGDMA) coated patches. Bars indicate SD and statistical significance was indicated with an asterisk (*p ≤ 0.05, **p ≤0.01, ***p ≤ 0.001) 12
Figure 6 Western blot result representing the protein uptake of BDCM cells.....14
Figure 7 ELISA result for HER2 and IGF-IR release from patches.....15
Figure 8 The amount of cytokines secreted by CD 4+ T cells.....16
Figure 9 Summary for types of photothermal agents and their photothermal conversion mechanism (Li et al., 2021) 19
Figure 10 Extinction coefficient diagram of tissue (Jaque et al., 2014) 20
Figure 11 Representation of Est/PD/RB-BT nanostructure.....21
Figure 12 The toxicity of Est/PD/RB-BT nanoparticles on MCF-7 cells. Bars indicate SD and statistical significance was indicated with an asterisk (*p ≤ 0.05, **p ≤0.01, ***p ≤ 0.001).....24
Figure 13 Toxicity of Est/PD/RB-BT nanoparticles on BEAS-2B cells. Bars indicate SD and statistical significance was indicated with an asterisk (*p ≤ 0.05, **p ≤0.01, ***p ≤ 0.001).....25
Figure 14 Confocal images for (A) MCF-7 cells, (B) MCF-7 cells incubated with PD/RB-BT, (C) MCF-7 cells incubated with Est/PD/RB-BT. (Red channel excitation: 561 nm, emission: 639 nm).....26
Figure 15 The change in cell viability following 0.04 and 0.08 mg/mL Est/PD/RB-BT and light treatment. Bars indicate SD and statistical significance was indicated with an asterisk (*p ≤ 0.05, **p ≤0.01, ***p ≤ 0.001) 27
Figure 16 Jablonski diagram that represents the PDT [Modified from: (Baskaran et al., 2018)].....30

Figure 17 a) The RB molecular structure and representation of $^1O_2$ generation (Sztandera et al., 2021) b) UV absorption spectra of RB (Nsubuga et al., 2021).....31
Figure 18 Crystal structure of BT a) Rhombohedral, b) Orthorhombic, c) Tetragonal, d) Cubic, e) Hexagonal (Lacerda et al., 2015) 32
Figure 19 The change in MCF-7 cell viability upon treatment with RB-BT nanostructures and fs laser treatment. 35
Figure 20 The change in MCF-7 cell viability upon treatment with Est/PD/RB-BT nanostructures and combined laser irradiation. 36

LIST OF SYMBOLS AND ABBREVIATIONS

$^1O_2$	Singlet Oxygen
BT	Barium Titanate
CD	Cluster of Differentiation
CW	Continuous Wave
DDS	Drug Delivery System
DMEM	Dulbecco's Modified Eagle Medium
EGFR	Epidermal Growth Factor Receptor
ER+	Estrogen Receptor Positive
Est	Estrogen
FBS	Fetal Bovine Serum
FDA	Food and Drug Administration
Fs	Femtosecond
HER2	Human epidermal growth factor receptor 2
IFN	Interferon
IGF-1	Insulin-like Growth Factor 1
IGF-IR	Insulin-like Growth Factor 1 Receptor
IL	Interleukin
IV	Intravenous
MHC	Major Histocompatibility Complex
NIR	Near Infrared
Np	Nanoparticle
PCL	Polycaprolactone
PD	Polydopamine
PDT	Photodynamic Therapy
PEG	Polyethylene Glycol

PEO	Polyethylene Oxide
PLA	Polylactic Acid
PLGA	Poly Lactic-co-Glycolic Acid
PR	Progesterone Receptor
PS	Photosensitizer
PTT	Photothermal Therapy
RB	Rose Bengal
ROS	Reactive Oxygen Species
RTK	Receptor Tyrosine Kinase
SHG	Second Harmonic Generation
Th1 / Th2	T Helper Type 1 or 2
TNF	Tumor Necrosis Factor
iCVD	Initiated Chemical Vapor Deposition
SD	Standard Deviation
US	Ultrasound

CHAPTER 1: INTRODUCTION

1.1. Breast Cancer and Current Treatment Methods

Breast cancer is one of the most prevalent causes of death by cancer in women. Only in 2020, there were 2.3 million women diagnosed with breast cancer, and 685,000 death was recorded worldwide (WHO, 2021). It is categorized according to the overexpression of hormone receptors: HER2+, luminal A, luminal B, and triple-negative (Alamdari et al., 2022). Luminal A subtype defines a patient profile whose tumor cells overexpress ER and/or PR but not HER2, whereas Luminal B tumor cells overexpress ER and/or PR as well as HER2. 70-75 % of breast cancer are linked to the overexpression of ER (Mayrovitz, 2022). HER2 overexpression is known to be an aggressive subtype, it is encountered in 20-25% of the overall cases (Park et al., 2022). Triple-negative breast cancer, on the other hand, does not overexpress any of the aforementioned hormone receptors.

The current treatment modalities for breast cancer include surgery, radiotherapy, chemotherapy, immunotherapy, endocrine therapy, and targeted therapy (Costa et al., 2020). Although these methods demonstrate remarkable results, most of them carry the disadvantage of affecting healthy cells besides cancerous cells. The reason behind this nonspecific uptake is that the therapeutics are usually administered intravenously, thus, they exert a systemic effect rather than a localized effect in the body (Moorthi et al., 2011).

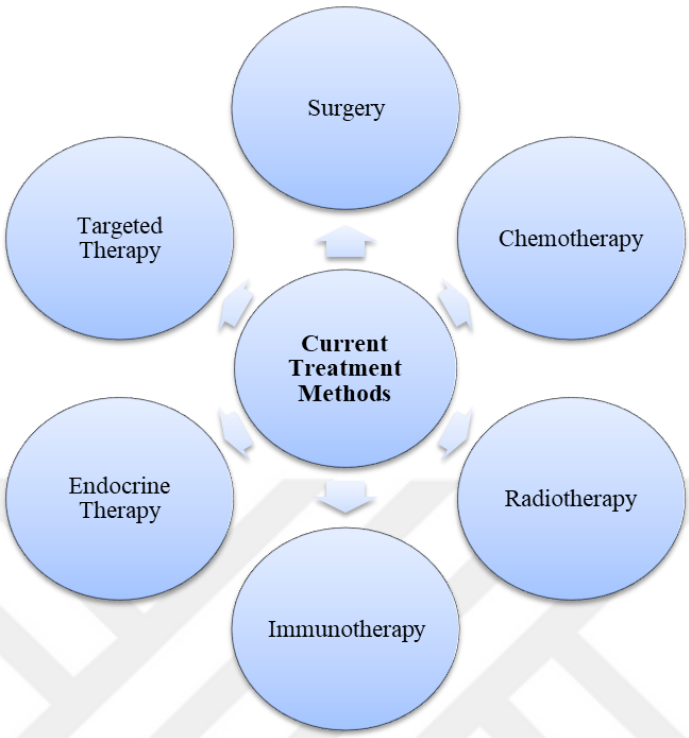

Figure 1 Current treatment methods for breast cancer

1.2. Localized Treatment for Breast Cancer

Compared to systemic delivery, localized delivery brings the advantage of the administration of therapeutics directly to the site of disease, and thus minimizes the risk of affecting the healthy cells and increases the dose received by the tumor cells. In localized therapy, therapeutics are usually administered to the site of the disease through an implantable device (Chew & Danti, 2017).

Among the different alternatives in implantable devices, nanofiber-based DDSs hold the advantage of controlled release through the adjustment of the composition, morphology, and porosity of the fibers (Jayakumar et al., 2010). They have been widely studied for the treatment of breast cancer over the years (X. Li et al., 2020; Akpan et al., 2020; Sedghi et al., 2017; Soukasene et al., 2011). Usually, biodegradable polymers such as PLGA, PCL, PEO, PEG, and PLA are used for the production of nanofiber-based implantable devices. They are

studied more widely compared to their non-biodegradable counterparts as they can degrade inside the body and thus eliminates the need for additional surgery.

Recently, phototherapy, which is a light-mediated treatment modality, gained increased attention for the localized treatment of cancers (Zhou et al., 2020). PDT and PTT being two types of phototherapy, they function through the activation of a light-responsive material upon suitable light irradiation. Once irradiated by a light source, these materials either cause hyperthermia or generate ROS that induce cell death in PTT and PDT, respectively. Their uses in the treatment of breast cancer have also been widely investigated (Higbee-Dempsey et al., 2019; Cai et al., 2020; Buchner et al., 2019; Mfouo-Tynga et al., 2018). These treatment methods usually combine the use of phototherapy with conventional treatment methods such as surgery and chemotherapy (Lamberti et al., 2014).

The choice of treatment modality is also highly affected by metastasis as it is a major problem associated with cancer. Surgery is a helpful method in the prevention of cancer metastasis to a remote site if the cancer is in its early stages (Lee et al., 2017). For the later stages, however, this strategy might be insufficient and there might be tumor cells left at the surgery site which can lead to metastasis or local recurrence (Pial et al., 2022). Thus, surgery is used in combination with other therapeutic approaches to increase the effectiveness of the treatment. Research that targets metastatic breast cancer has been conducted (Shi et al., 2020; Kefayat & Vaezifar, 2019; Li et al., 2020). Successful treatment modalities included the implantable DDS, and they demonstrated decreased levels of recurrence and metastasis especially in the lungs which is one of the most common metastatic sites for breast cancer (Grobmyer et al., 2012).

1.3. Aim of the Study

In this thesis, the *in vitro* effect of a polymeric nanofiber-based DDS that was previously designed by using breast cancer as model was investigated. ER and HER2 overexpression define a major part of breast cancer cases (Gutierrez & Schiff, 2011). This DDS is composed of a HER2 and IGF-IR incorporated PLGA patch that is produced by blowspinning technique, and NIR-responsive nanoparticles that are produced by using ER+ breast cancer as target disease (Figure 2). The aim of this DDS is to provide an efficient therapeutic alternative and prevent the recurrence and metastasis by (i) releasing HER2 and IGF-IR proteins incorporated inside this patch to activate the immune system (ii) releasing NIR-responsive nanoparticles to create a combined photothermal and photodynamic effect that triggers the death of remaining tumor cells at the surgery site. First, the findings regarding the *in vitro* effect of the protein-incorporated polymeric platform, then the *in vitro* effect of NIR-responsive nanostructures is presented.

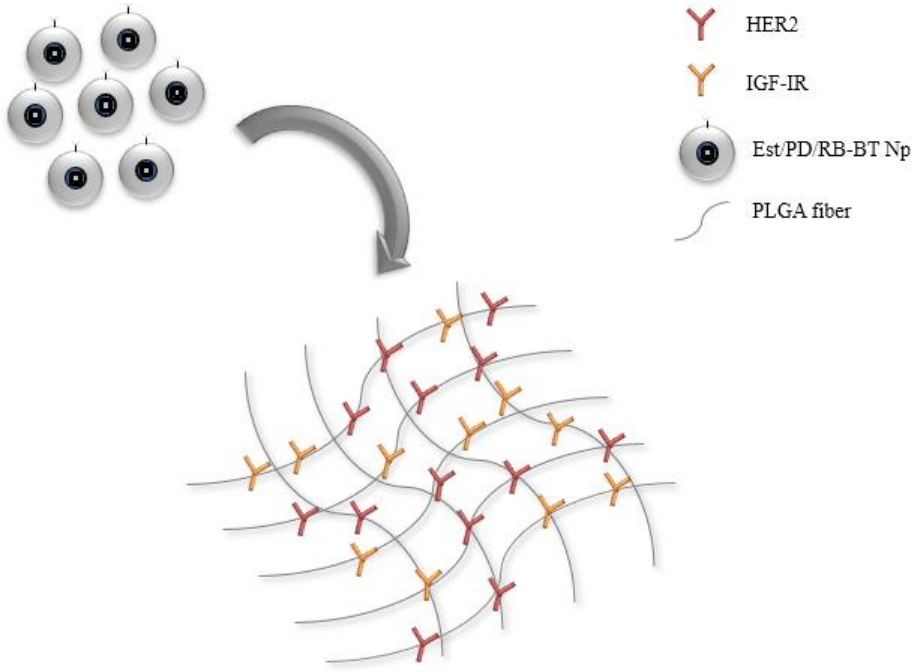

Figure 2 Representation of DDS

CHAPTER 2: INVESTIGATION OF THE *IN VITRO* EFFECT OF HER2 AND IGF-IR INCORPORATED IMPLANTABLE PATCHES

2.1. Introduction

2.1.1. Implantable DDSs

Most of the conventional methods for the treatment of cancer lack site specificity and deliver therapeutic to the whole body. This systemic delivery has the drawback of off-target uptake by the healthy tissue and lowered therapeutic concentration at the target site (Chew & Danti, 2017). The localized treatment modalities overcome these drawbacks by the administration of the therapeutics directly to the site of the disease.

One such treatment modality is the implantable devices which are designed to be implanted directly to the site of disease. Many different agents such as drugs, proteins, and even cells can be incorporated into their structure according to the application purposes. They can be either preformed or *in situ* forming (Hope et al., 2022). Preformed implantable DDSs are more advantageous as they provide a wide range of fabrication methods and enable more control over the DDS features. Among different types of preformed DDSs, fiber-based ones have been emerging due to the advantages they provided such as providing controlled release of the incorporated agents. Usually, biodegradable polymers such as PLGA, PLA, and PVA are used as they can degrade in the body and do not require surgery for the removal.

Controlled release is an important feature of a DDS as it enables keeping the administered concentration at the therapeutic window level and supplies the therapeutic to the site of

disease for an extended period of time (Agrawal H et al., 2011). It also reduces the risk of toxicity to healthy cells (Hussain et al., 2022). Stimuli-responsive biomaterials are widely used to control the release of therapeutics. They function upon activation by endogenous, such as enzyme and pH; or exogenous stimuli, such as temperature, light, and US (Raza et al., 2019). The integration of stimuli-responsive biomaterials to the DDSs can be achieved via different means. One such strategy is the coating of implantable DDS by iCVD method (Gleason, 2021).

2.1.2. The Relationship of Breast Cancer with HER2 and IGF-IR

RTK is a group of transmembrane receptors that play an important role in signal transduction. They are involved in many cellular processes including proliferation, differentiation, metabolism, death, and oncogenesis (Sudhesh Dev et al., 2021), (Sapra Sharma et al., 2009). The EGFR, or ErbB, growth factor receptors are a group of RTK that includes HER1, HER2, HER3, and HER4 in humans. Among the ErbB family, the overexpression and activation of HER1 and HER2 are linked to the development of several types of cancer (Cho & Leahy, 2002). Furthermore, HER2 overexpression is related to approximately 20% of breast cancer cases (Gutierrez & Schiff, 2011).

IR is another group of RTK that includes IGF-IR. Upon activation by IGF-I, IGF-IR triggers several cellular processes such as proliferation, protein synthesis, glucose and lipid metabolism, regulation of gene expression, and death (Boucher et al., 2010). Overexpression of IGF-IR and the malignant transformation of the cells are correlated and thus it is linked to several types of cancer including breast cancer (Ward C et al., 2000; Jones et al., 2007). Research demonstrated that IGF-IR levels showed a 14-fold increase in human breast cancer cells.

2.1.3. Activation of Adaptive Immune System

The immune system plays an essential role in defending the host against invading pathogens. While the first and fastest response against pathogens is accomplished by innate immunity, sometimes the defense mechanism established by the innate immune system becomes insufficient in the recognition of pathogens (Janeway CA Jr et al., 2001). The adaptive immune system is tailored to generate antigen-specific immune responses and thus provides an enhanced protection mechanism against pathogens.

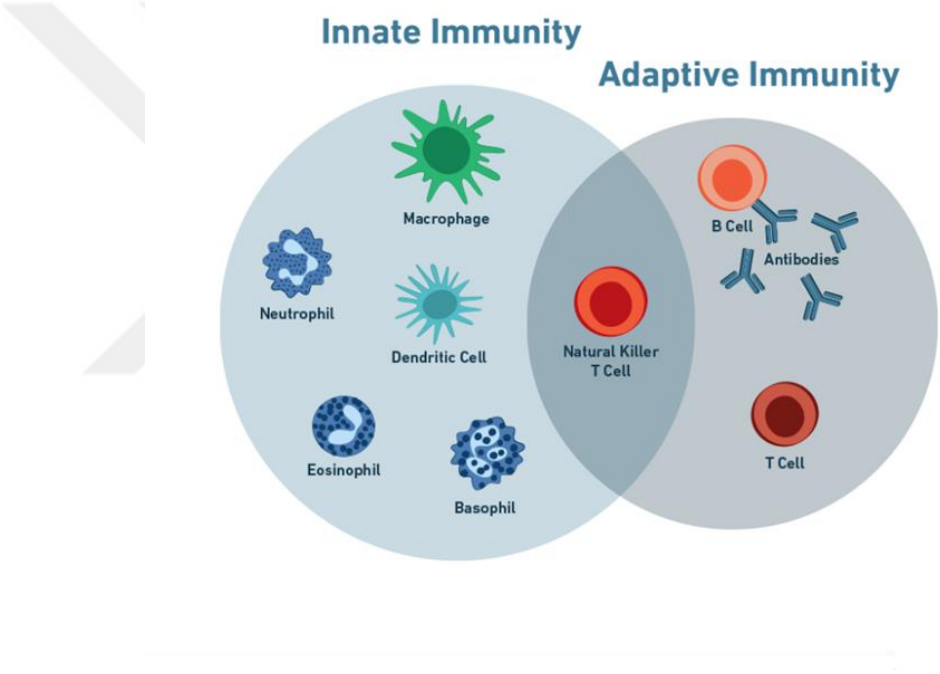

Figure 3 Schematic representation of the immune system (Lowell, 2020)

The adaptive immune response is initiated by the phagocytosis of pathogens by immature dendritic cells. Following phagocytosis, the dendritic cell is activated and the proteolyzed antigens are loaded to the MHC molecules present on the surface of dendritic cells. Then, the dendritic cells travel to the regional lymph node where they present the antigens to T lymphocytes and activate them, which is also called T cell priming.

CD 4+ and CD 8+ T cells constitute the majority of T lymphocytes. CD 4+ T cells, also known as T helper cells, contribute to the generation of adaptive immune response by the

secretion of cytokines upon the presentation of the antigens by dendritic cells (Luckheeram et al., 2012). According to the released cytokines, which are the important signaling proteins of the immune system, the CD 4+ T cells are divided into different subsets. Th1 and Th2 being two of these subsets, Th1/Th2 ratio is a representation of the balance of immune response (Liew F. Y., 2002). Th1 cells secrete cytokines including IL-1β, IL-2, IL-12, TNF-α, and IFN-γ, and their secretion is related to immune system activation. On the other hand, the secretion of Th2 cytokines, IL-4, IL-5, and IL-10, is correlated with the suppression of the immune response which results in tumor growth in cancer cases (Lee et al., 2019).

2.1.4. Aim of the study

The aim of the study is to investigate the effect of the HER2 and IGF-IR incorporated PLGA patches on the immune cells and evaluate the success in the induction of immune response by presenting HER2 and IGF-IR proteins as “antigens” to the T helper cells.

2.2. Materials and Methods

2.2.1. Materials

RPMI-1640 (ATCC), FBS Premium (Pan Biotech), WST-8 Kit (Sigma Aldrich), TNF-α, IFN-γ ELISA Kit, IL-2, IL-4 ELISA Kit (Peprotech, 900-TM27, 900-TM12, 900-TM14, 900-TM25).

2.2.2. Methods

2.2.2.1. Cell culture

BDCM (B cells with Dendritic Cell Morphology, ATCC) and Primary CD 4 + T cells (ATCC) were prepared for the experiments starting from passage 0. Both the cells were maintained in RPMI-1640 medium containing 10% FBS.

2.2.2.2. Investigation of Patch Cytotoxicity

The patch toxicity was evaluated by WST-8 method. The BDCM cells were seeded in a 24-well plate at a density of 5,000 cells/ 100 µl. The patches of 1 cm x 1 cm dimensions were inserted in each well, except for the well in which the control group exists. Before introducing the patches to the *in vitro* environment, they were sterilized under a UV lamp for 10 minutes. In order to evaluate the toxicity of patches over a time period of 1, 3, or 7 days, the plates were incubated at 37º C and %5 CO_2 environment. On their day 3, fresh medium was introduced to the cells that were incubated with patches for 7 days. Following 1,3 and 7 days of incubation, the cells were transferred to a 96-well plate so that there were 100 µl of cell suspension/well. Then, 10 µl of CCK-8 solution was added to each well. After 4 hours of incubation in the dark, the OD values were measured at 450 nm by microplate reader (Tecan Infinite m200 Pro).

2.2.2.3. Investigation of HER2 and IGF-IR Loading of BDCM Cells

HER2 and IGF-IR uptake of BDCM cells was evaluated by western blot analysis. Prior to western blot, the patches of 1 cm x 1 cm dimensions were sterilized under UV lamp for 10 minutes, and then they were introduced to the BDCM cells seeded to a 24-well plate with a density of 250,000 cells/well. Following 24 hours of incubation at 37º C and 5% CO_2

environment, the cell suspension was centrifuged, and the cell pellets were obtained for western blot analysis.

2.2.2.4. Assessment of the Immune System Activation

In order to observe the success of the patches in the stimulation of immune cells, ELISA was conducted to evaluate whether the TNF-α, IFN-γ, IL-2, and IL-4 cytokines were produced or not. Prior to the ELISA, BDCM cells were cultured with patches for 24 hours by following the same protocol as in the western blot analysis. Then, the patches were removed and the primary CD 4+ T cells were introduced to the medium so that the ratio between the BDCM and CD 4+ T cells is 1:4 (Kharbanda et al., 2002). After 24 hours of coculture, the cell suspension was centrifuged to obtain the medium that will be used in the ELISA. The ELISA protocol for TNF-α, IFN-γ, IL-2, and IL-4 cytokines being the same, the assay was conducted by following the manufacturer's instructions.

2.3. Results and Discussion

2.3.1. Investigation of Patch Cytotoxicity

Within the scope of the patch cytotoxicity investigation, PLGA patches that possess different properties were evaluated using BDCM cells. The preliminary studies were conducted with uncoated PLGA 65:35 patches. Then, the studies were continued with both uncoated and pH-responsive poly (DMAEMA-co-EGDMA) coated PLGA 50:50 patches.

2.3.1.1. Uncoated Patch

For the uncoated PLGA patch cytotoxicity studies, the cytotoxicity of patches that do not contain any protein, and the patches that contain only HER2 were investigated. The

cytotoxicity of patches that were prepared with two different concentrations of HER2 was evaluated: 0.7 µg/mL and 1.4 µg/mL. The toxicity of the patches was observed following 1, 3, and 7 days of incubation with cells. The OD values measured by the microplate reader are a demonstration of cell viability. The graphs representing the variation in the viability with changing concentrations were created by taking the viability of the untreated group (control group) as 1-fold. The viability of the other experimental groups was calculated by comparing their OD values to that of the control group. The results are demonstrated in Figure 4.

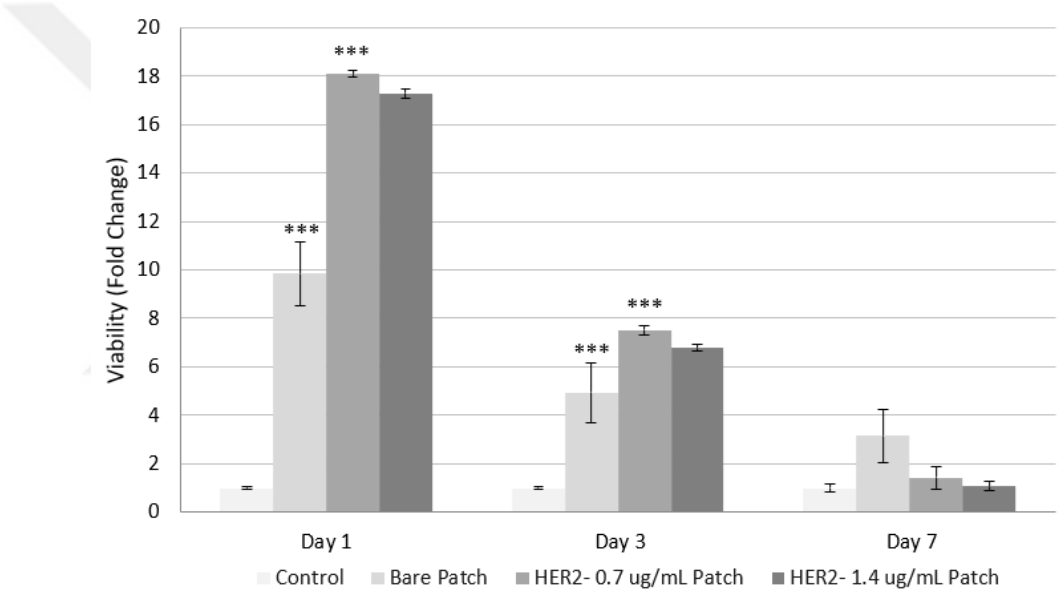

Figure 4 The change in cell viability across experimental groups at different time points. Bars indicate SD and statistical significance was indicated with an asterisk (*p ≤ 0.05, **p ≤0.01, ***p ≤ 0.001)

The results demonstrated that there was a significant increase in cell viability for all PLGA patches on day 1. The HER2-incorporated patches demonstrated increased viability compared to the bare patch, but the increased HER2 concentration showed decreased viability on BDCM cells. The same trend was observed on day 3 and day 7, however, for each time point, the viability increase demonstrated a decreasing trend compared to the previous time point. First, as the patch is without coating, the released amount of HER2 might decreased in time and this led to a diminished increase in cell viability. Second, the sharp

increase in cell viability due to boosted HER2 uptake by the cells might led to cell culture medium shortage, and thus the viability increase showed a decreasing trend.

The results demonstrated that the increased HER2 concentration resulted in decreased cell viability. Therefore, the amount of HER2 to be incorporated into the patches was optimized as 0.7 µg/mL.

2.3.1.2. Coated Patch

Upon the completion of preliminary studies with bare and HER2-incorporated PLGA 65:35 patches, the cytotoxicity studies of HER2 and IGF-IR incorporated PLGA 50:50 patches were conducted. The toxicity of poly (DMAEMA-co-EGDMA) coated patches by the iCVD technique was investigated.

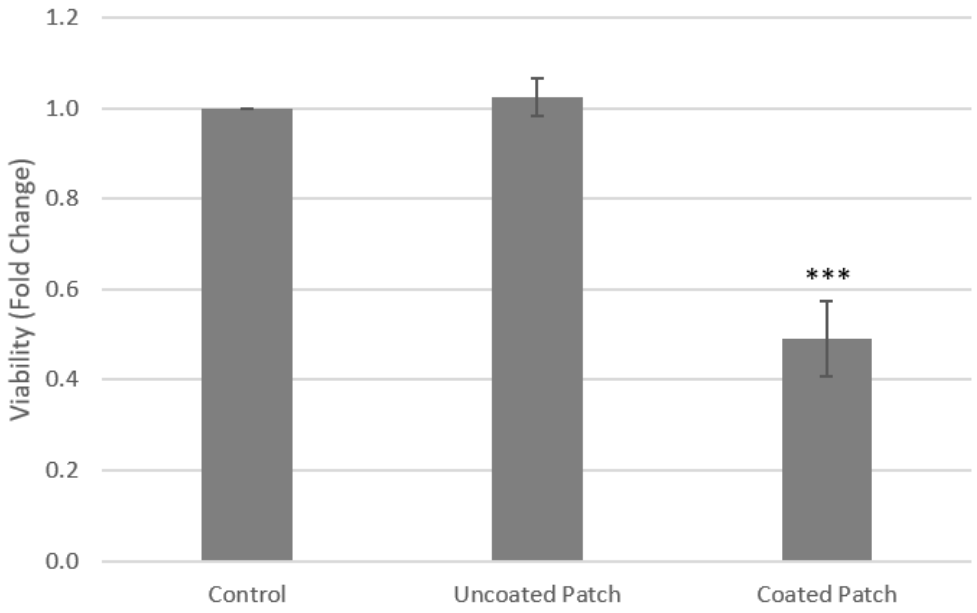

Figure 5 : The cytotoxicity of HER2 and IGF-IR incorporated uncoated, and poly (DMAEMA-co-EGDMA) coated patches. Bars indicate SD and statistical significance was indicated with an asterisk (*$p \leq 0.05$, **$p \leq 0.01$, ***$p \leq 0.001$)

Figure 5 shows that the uncoated PLGA 50:50 patch did not demonstrate any toxic effect on BDCM cells. However, the poly (DMAEMA-co-EGDMA) coated patches caused approximately a 50% decrease in cell viability. Acrylic acid monomers are known to induce cell apoptosis. They demonstrate this effect by their metabolism to the 2,3-epoxymethacrylic acid which is an epoxide that exerts a cytotoxic and genotoxic effect (Reichl et al., 2010). Therefore, the decreased viability might be attributed to the presence of methacrylic acid monomers EGDMA and DMAEMA. First, besides the successful poly (DMAEMA-co-EGDMA) coating, there might also be monomers deposited onto the patches that did not undergo the polymerization process. Second, the polymer coating might decompose its monomers inside the cell culture medium in the course of time.

2.3.2. Investigation of HER2 and IGF-IR Loading of BDCM Cells

The success of the BDCM in loading the antigens to the MCH Class II molecules was investigated by western blot analysis. Figure 6 depicts the film obtained from western blot analysis.

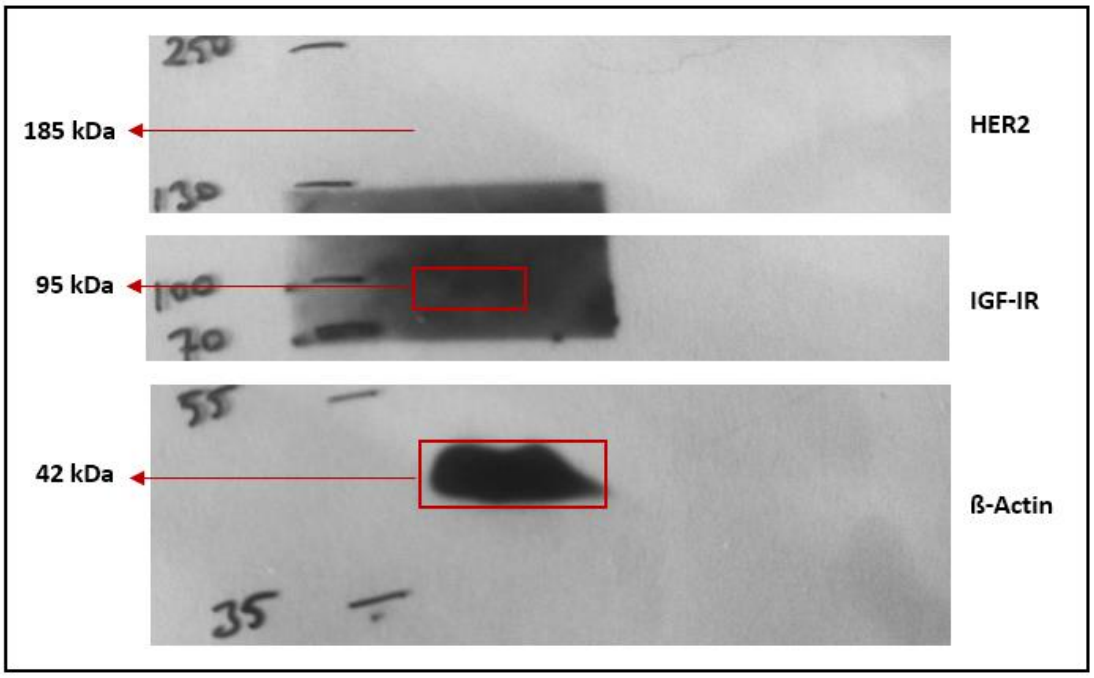

Figure 6 Western blot result representing the protein uptake of BDCM cells

The image illustrates the presence of the bands near 42 kDa, and 95 kDa. These bands correspond to the positive control β-actin and the IGF-IR, respectively. The bands corresponding to the HER2, at 185 kDa, were not observed. This observation agrees with what was observed by the results of ELISA conducted for the detection of the released amount of HER2 and IGF-IR proteins from the patches (Figure 7).

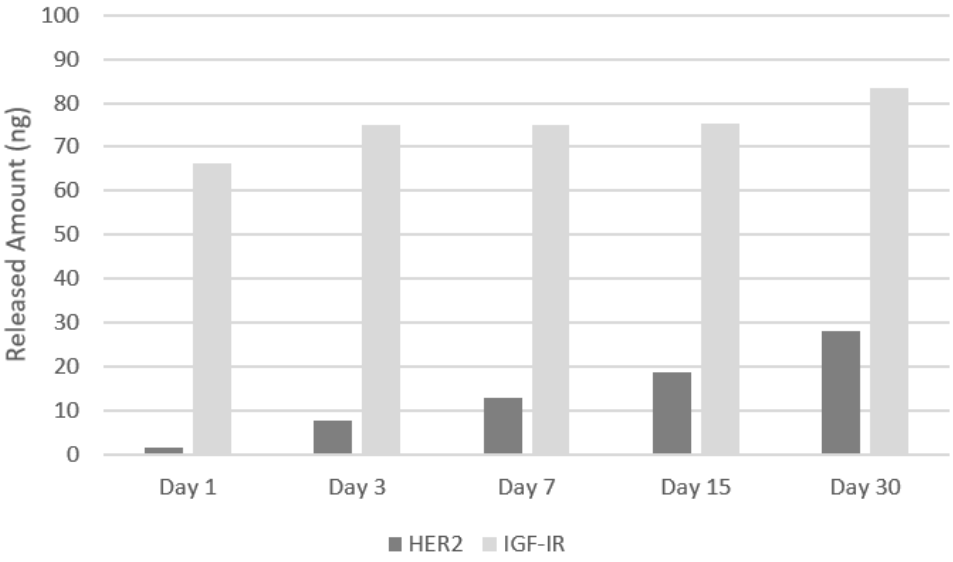

Figure 7 ELISA result for HER2 and IGF-IR release from patches

Although the western blot method is known to be useful in the protein detection through the specific binding of antibodies, the western blot might be a less sensitive method compared to the ELISA (Pestronk & Lopate, 2005). The detection limits of the western blot method start at the nanogram levels, and the detection depends heavily on the antibody affinity and the protein concentrations. On the other hand, the lower detection limit of the ELISA method is as low as a few picograms. Although HER2 could not be detected by western blot analysis, the results are coherent with what was obtained from ELISA. The amount of HER2 released at the end of day 1 was detected as 1.6 ng by the ELISA method. Therefore, the amount uptake and loaded by BDCM cells would be less than this amount which makes it difficult to be detected by western blot analysis.

2.3.3. Assessment of Immune System Activation

It was expected to observe the activation of CD 4+T cells upon antigen presentation by BDCM cells. In order to understand whether the antigens presented by BDCM cells have a stimulative or suppressive effect, the amount of TNF-α, IL-2, IL-4, and IFN-ɣ cytokines was detected by the ELISA method.

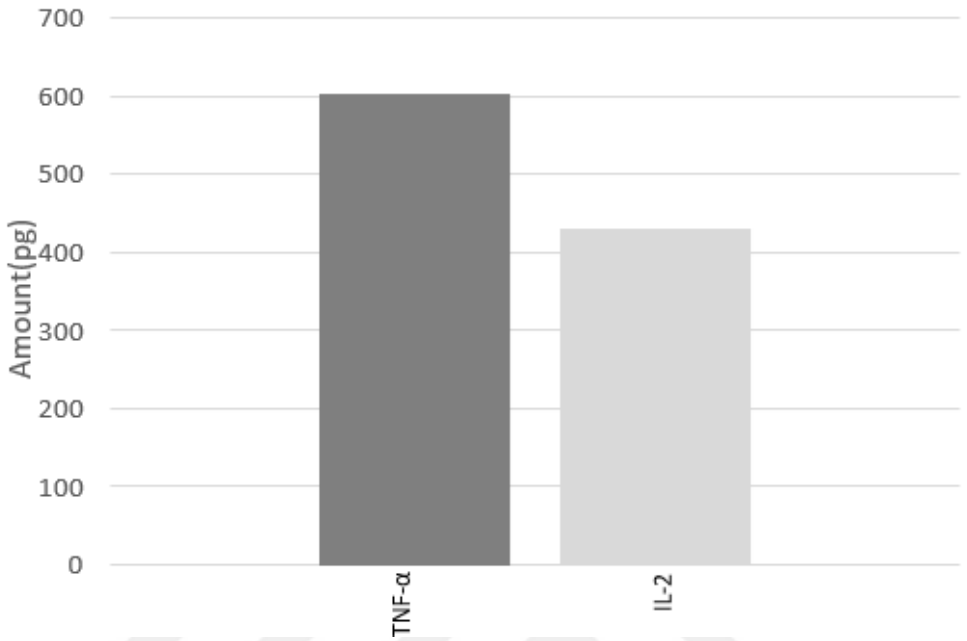

Figure 8 The amount of cytokines secreted by CD 4+ T cells

As it is represented in Figure 8, only the TNF-α and IL-2 cytokines were detected in the CD 4+ T cell culture medium whereas IFN-ɣ and IL-4 release were not detected. According to ELISA, the detected amounts of TNF- α and IL-2 cytokines are 602 and 430 ng, respectively. It is concluded that either the IFN-ɣ and IL-4 cytokines were not secreted by the CD4+ cells or the secreted amount was below the lower detection limit (2000-8 pg/mL) of the assay. Therefore, the amount of released cytokines by CD 4+ cells demonstrates that the TNF-α and IL-2 cytokines that trigger the immune systems are higher than that of the IL-4 cytokines. Thus, the detection of TNF-α and IL-2 cytokines was attributed to the stimulation of immune cells by HER2 and IGF-IR epitopes.

2.4. Conclusion

The interaction of the IGF-IR and HER2-incorporated PLGA patches with immune cells was investigated. Neither of the PLGA 65:35 and 50:50 patches without coating showed toxic

effect, whereas the poly (DMAEMA-co-EGDMA) coated patches demonstrated a toxic effect on BDCM cells. The western blot analysis demonstrated only the uptake of IGF-IR by BDCM cells. That is attributed to the lower amount of HER2 release compared to the IGF-IR release that was investigated by ELISA. Detection of TNF-α and IL-2 cytokines revealed that the immune system was triggered by HER2 and IGF-IR-incorporated implantable patches.

CHAPTER 3: INVESTIGATION OF THE *IN VITRO* EFFECT OF NIR-RESPONSIVE NANOSTRUCTURE

3.1. Introduction

Phototherapy is a therapeutic modality in which the treatment is achieved through a light source. It finds its application in the treatment of various diseases such as skin conditions and cancer types (Wong et al., 2013; Shibu et al., 2013; Ramasethu, 2004; Szeimies et al., 2005). PTT and PDT are two types of phototherapy that show their effect through the use of therapeutics that can respond to suitable light irradiation. In this context, a variety of nanomaterial formulations have been developed to increase the therapeutic efficacy of PDT and PTT. In this chapter, the details regarding the PTT will be introduced. The information regarding the PDT will be introduced in Chapter 4.

3.1.1. Photothermal Effect and PTT

PTT is a light-mediated therapy in which a light-absorbing material, also called photothermal material, is used to generate localized heat to trigger cell death at the site of the disease. Upon their irradiation, the photothermal materials are transferred to an excited state. As they return to their ground state, a fraction of the absorbed energy is released through non-radiative relaxation and generates heat. The amount of released heat depends on the photothermal conversion efficiency and the absorption performance of the material (An et al., 2023).

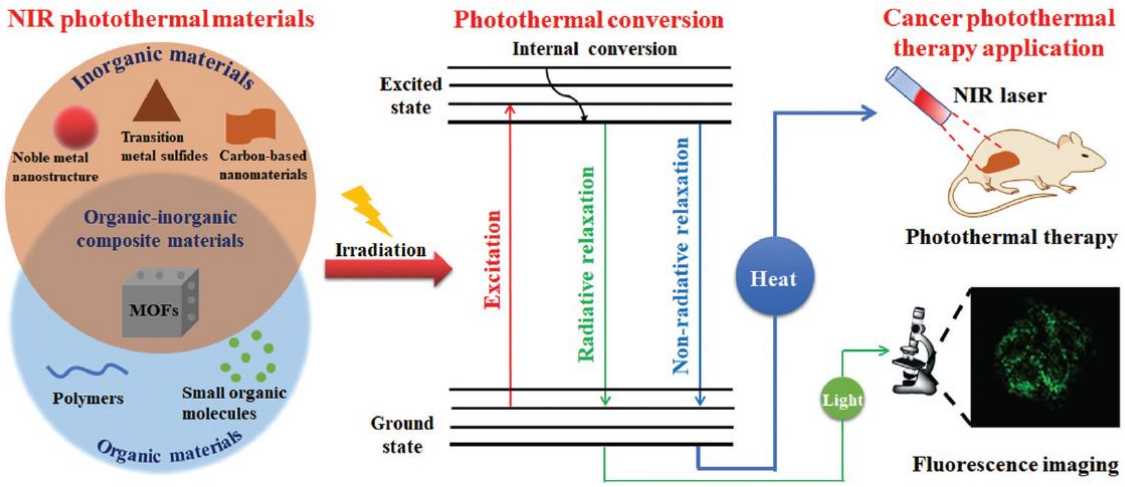

Figure 9 Summary for types of photothermal agents and their photothermal conversion mechanism (Li et al., 2021)

Usually, the agents that can be excited with a NIR light source in the wavelength range correspond to the biological windows are used for the photothermal treatment (Jaque et al., 2014). The tissue is partially transparent at the spectral ranges of 700-980 nm and 1000-1400 nm which are called first and second biological windows, respectively. This transparency is brought by the reduction in the absorption of constituents such as hemoglobin and water and scattering within the tissue. Operation at these wavelengths helps reach deeper regions within the tissue and prevents the heating of healthy tissue.

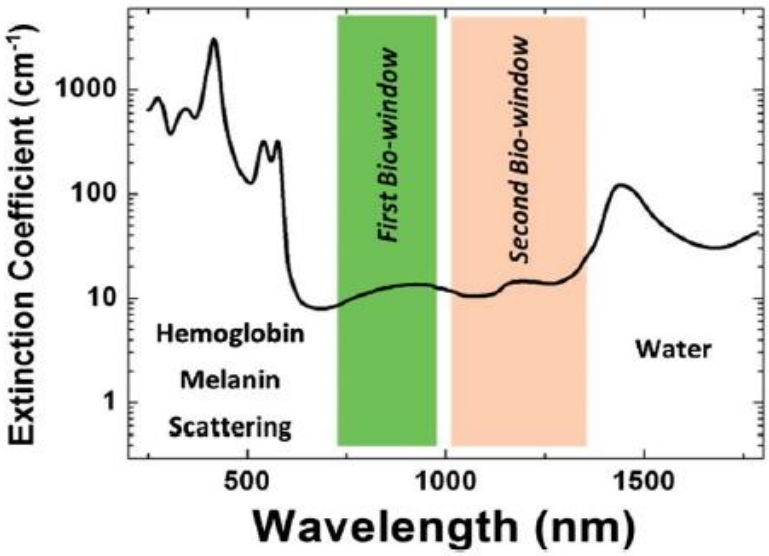

Figure 10 Extinction coefficient diagram of tissue (Jaque et al., 2014)

An efficient photothermal agent should have a high absorption coefficient and low luminescence quantum yields as this will enable a higher conversion efficiency from light to heat (Jaque et al., 2014).

Dopamine is a catecholamine that is released by the central nervous system to function as a neurotransmitter. It can undergo the self-polymerization reaction in an alkali environment to form PD that presents surface-adhesive properties. PD has been widely used in the coating of nanomaterials as they provide the advantage of high circulation time upon IV injection due to their stabilities (M. Li et al., 2018). It also holds the advantage of low toxicity and strong NIR absorption. They are also widely studied in anti-cancer treatment by making use of their photothermal conversion efficiency (Fan et al., 2022).

3.1.2. Aim of the study

The NIR-responsive nanostructure, called EST/PD/RB-BT, is depicted in Figure 11. The EST/PD/RB-BT nanostructure is aimed to be used in the combined photothermal and photodynamic treatment of ER+ breast cancer in a site-specific manner.

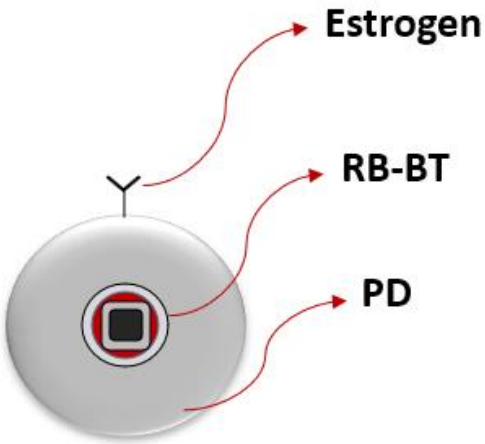

Figure 11 Representation of Est/PD/RB-BT nanostructure

The nanoparticle complex includes RB-BT to create the photodynamic effect; PD as the photothermal agent and Estrogen to introduce the site-specificity.

The aforementioned advantages possessed by the PD make it a good alternative to both achieve a photothermal effect and to encapsulate another therapeutic inside, *i.e.*, RB-BT, to deliver it to the diseased site. The rationale behind the integration of RB-BT into the nanoparticle structure will be introduced in Chapter 4.

3.2. Materials and Methods

3.2.1. Materials

DMEM (Pan Biotech), FBS (South America, Pan Biotech), L-glutamine (Pan Biotech), Penicillin-Streptomycin (100X) (Pan Biotech), Trypsin-EDTA (Pan Biotech), Phosphate Buffered Saline (1X) (Pan Biotech), WST-8 Kit (Sigma Aldrich), Hoechst 33342 (Invitrogen).

3.2.2. Methods

3.2.2.1. Cell culture

The MCF-7 (Human ER+ breast cancer cell line) and the BEAS-2B (Human lung epithelial cell line) were used for the experiments. MCF-7 cells were maintained in DMEM containing % 10 FBS and %1 Pen-Strap in a 5% CO_2 and 37º C environment. BEAS-2B cells were maintained in DMEM supplemented with 20% FBS and %1 Pen-Strap.

3.2.2.2. Dark Toxicity of Est/PD/RB-BT

The cell viability of MCF-7 cells was evaluated through WST-8 assay following the manufacturer's instructions. Briefly, 5 x 10^3 cells were seeded in 96 well-plate and incubated for 24 hours at 37º C and 5% CO_2 environment. Then, the medium was replaced with a fresh medium containing Est/PD/RB-BT particles at different concentrations (0.01, 0.02, 0.04, 0.08 mg/mL) and incubated for 24 or 72 hours. Following the incubation, the medium was replaced with fresh medium, and %10 of the CCK-8 solution was introduced. After 3 hours of incubation in the dark, the OD values were measured with a microplate reader (Tecan Infinite m200 Pro) at 450 nm wavelength.

3.2.2.3. Cellular Uptake

The cellular uptake of Est/PD/RB-BT particles by MCF-7 cells was investigated by confocal microscopy. The cells were seeded on coverslips at a density of 1 x 10^4, and incubated for 24 hours in a 5% CO_2 and 37º C environment. Then, the cells were treated with Est/PD/RB-BT nanoparticles. After 12 hours of incubation, cells were washed with PBS, and fixed with 4% Paraformaldehyde. Following 20 minutes of fixation, the cells were washed with PBS thrice, and the nucleus was stained with Hoechst 3342 (1 μg/mL). After 5 minutes of incubation, samples were washed with PBS thrice. Coverslips were mounted using 1:1 glycerol: PBS solution and the samples were investigated by confocal microscopy (Zeiss LSM 710).

In order to evaluate the increased site-specificity brought by the integration of estrogen to the nanostructure, the same procedure was followed by using the same concentration of PD/RB-BT instead of Est/PD/RB-BT.

3.2.2.4. Investigation of Photothermal Effect *In Vitro*

The photothermal effect of the Est/PD/RB-BT particles on MCF-7 cells was evaluated upon irradiation with an 808 nm CW laser. The cells were seeded in two different 96-well plates at a density of 1 x 10^4 cells/well for 24 hours. Then, the medium was replaced with fresh medium containing Est/PD/RB-BT nanoparticles (0.04, or 0.08 mg/mL). Following 24 hours of incubation, the cells in one of the plates were irradiated with an 808 nm continuous wave laser (1.5 W) for 30 minutes, whereas the other plate was not irradiated. Upon the completion of laser irradiation, the plates were incubated for 24 hours, and the same WST-8 protocol that was followed for the dark toxicity assay was applied for the assessment of the photothermal effect on MCF-7 cells.

3.3. Results and Discussion

3.3.1. Dark Toxicity of Est/PD/RB-BT

Figure 12 and Figure 13 demonstrate the effect of the increased Est/PD/RB-BT concentration on MCF-7 and BEAS-2B cells, respectively. For the data evaluation, the procedure explained in Chapter 2.2.2 was followed.

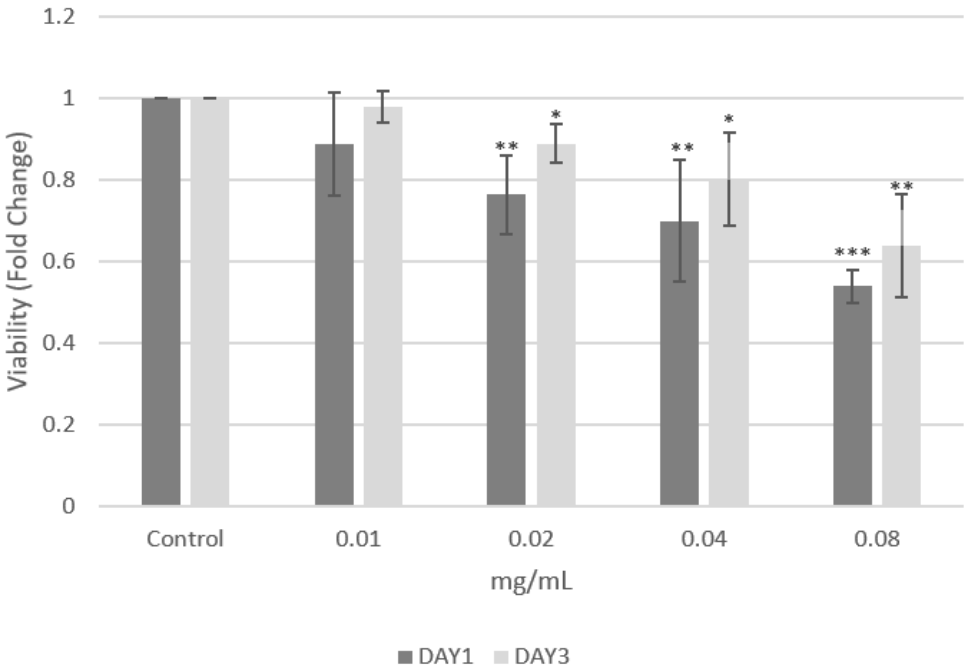

Figure 12 The toxicity of Est/PD/RB-BT nanoparticles on MCF-7 cells. Bars indicate SD and statistical significance was indicated with an asterisk (*p ≤ 0.05, **p ≤0.01, ***p ≤ 0.001)

As the concentration of Est/PD/RB-BT nanoparticles increased from 0.01 to 0.08 mg/ml, the MCF-7 cell viability decreased both on day 1 and day 3. However, the viability of MCF-7 cells showed an increase from day 1 to day 3 for each concentration. The increased viability for each Est/PD/RB-BT concentration from day 1 to day 3 is attributed to the estrogen that is attached to the nanoparticle structure for site-specific delivery of the Est/PD/RB-BT.

It is important that a therapeutic dose does not show a toxic effect on healthy cells. Therefore, in order to understand the effect of different Est/PD/RB-BT concentrations on healthy cells, the BEAS-2B cell line was used. The results are shown in Figure 13.

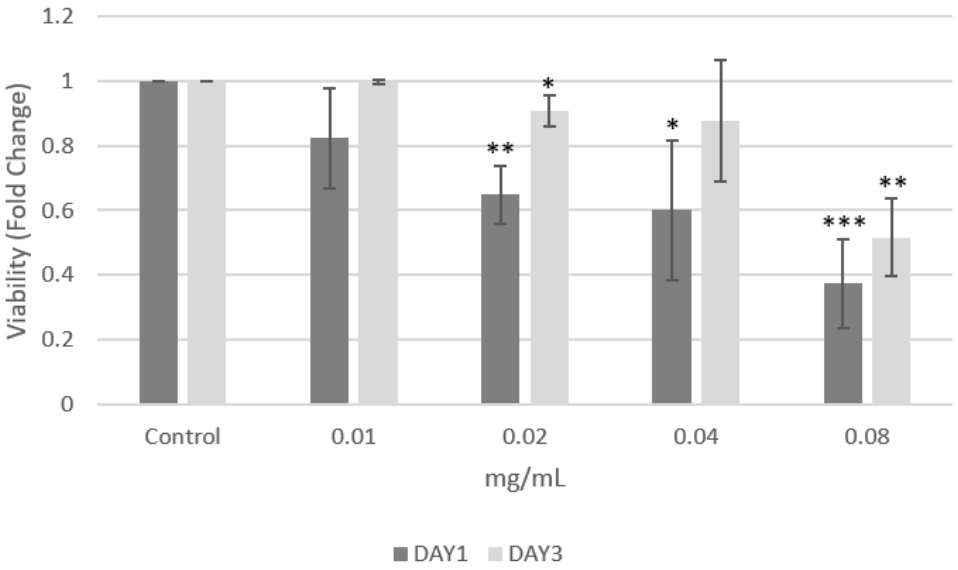

Figure 13 Toxicity of Est/PD/RB-BT nanoparticles on BEAS-2B cells. Bars indicate SD and statistical significance was indicated with an asterisk (*p ≤ 0.05, **p ≤0.01, ***p ≤ 0.001)

The cell viability increased from day 1 to day 3 for each concentration, as it was observed on the MCF-7 cells. However, compared to the MCF-7 cell line, the viability of BEAS-2B cells decreased more with increased concentration. The viability of both the cell lines was similar for 0.01 mg/mL concentration, whereas the viability of BEAS-2B cells decreases more starting with 0.02 mg/mL concentration as the normal cells are affected more by the chemicals compared to the tumor cells (Caroline & Rekha, 2022).

3.3.2. Cellular Uptake

The uptake of the PD/RB-BT and Est/PD/RB-BT particles by MCF-7 cells was investigated by confocal microscopy. As the RB possesses intrinsic fluorescence properties, it enabled the investigation of particle uptake by MCF-7 cells without needing any additional process for particle labeling. Untreated MCF-7 cells were used as the control group. The imaging settings for both the control and experimental groups were kept the same during the imaging process.

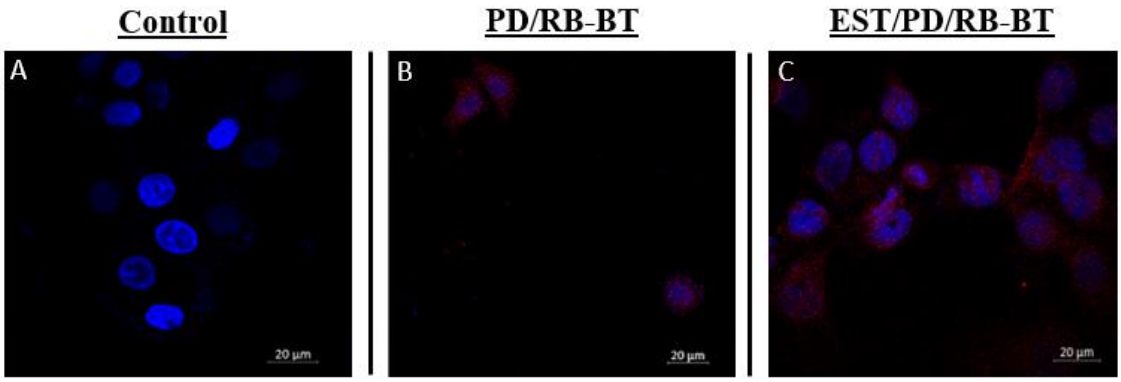

Figure 14 Confocal images for (A) MCF-7 cells, (B) MCF-7 cells incubated with PD/RB-BT, (C) MCF-7 cells incubated with Est/PD/RB-BT. (Red channel excitation: 561 nm, emission: 639 nm)

In Figure 14, the red signal indicates the presence of RB near the nucleus. Therefore, it also indicates that the PD/RB-BT and Est/PD/RB-BT nanoparticles were uptake by the MCF-7 cells.

Our preliminary studies demonstrated that for 3 hours and 6 hours of incubation, the uptake levels were not significant. The uptake of nanoparticles was observed after 12 hours of incubation of cells with particles. Our Est/PD/RB-BT nanoparticles possess a negative surface charge and have a diameter of 360 nm. Surface charge and the size of the particles are important parameters in their cellular uptake mechanism (Behzadi et al., 2017). The uptake percent of the particles possessing positive surface charge is higher than their negatively charged counterparts. In addition, particles as large as 300 nm demonstrate a slower uptake rate compared to particles possessing smaller sizes (Shapero et al., 2011). Therefore, the reason for the observation of the particles starting from the 12 hours but not in the earlier time points might be attributed to their size and surface charge.

The cells at the different locations of the microslide were investigated and the cells with red signal and without red signal were identified, their ratio was used for the quantification. The results obtained by the imaging of the cells incubated with PD/RB-BT and Est/PD/RB-BT

concluded that the integration of estrogen to the nanostructure resulted in an approximately 70% increase in the particle uptake.

3.3.3. Investigation of Photothermal Effect *In Vitro*

PD particles within the structure of Est/PD/RB-BT are known to cause hyperthermia and thus the ROS production that drives the cells to death (Dong et al., 2016). In order to evaluate the photothermal effect triggered by nanoparticles, three different experimental groups were investigated by comparing their viability to the control group, which is the cell that is neither treated with nanoparticles nor with laser. The results are shown in Figure 15. The viability of the experimental group treated with the particles is shown as "Nanoparticle Only", the group treated with laser is shown as "Laser Only", and the group treated both with nanoparticle and the laser is shown as "Nanoparticle and Laser" in Figure 15.

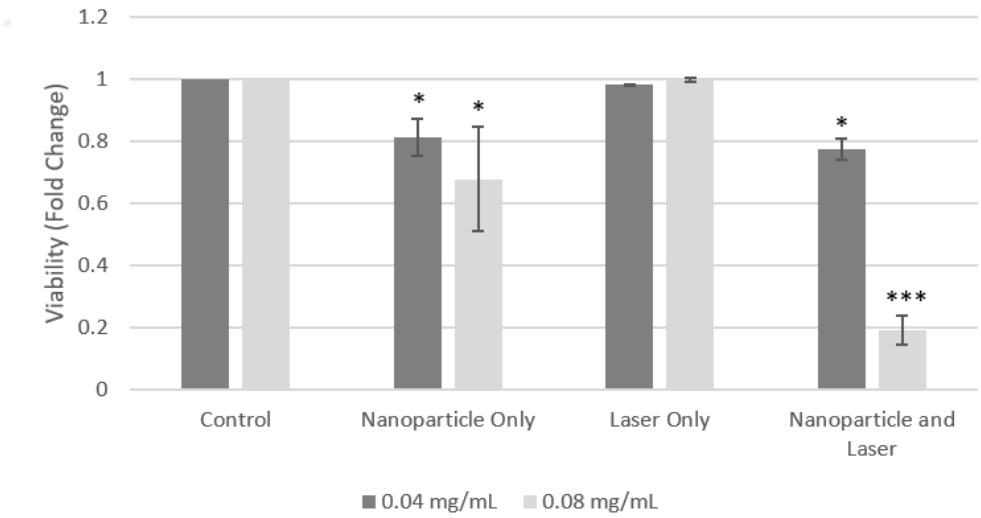

Figure 15 The change in cell viability following 0.04 and 0.08 mg/mL Est/PD/RB-BT and light treatment. Bars indicate SD and statistical significance was indicated with an asterisk (*$p \leq 0.05$, **$p \leq 0.01$, ***$p \leq 0.001$)

In the case of the cells treated with only 0.04 mg/mL nanoparticle, the viability decreased to 80% whereas the viability decreased to 70% for the experimental group treated with 0.08 mg/mL nanoparticle. The laser irradiation alone did not have an effect on the cell viability in

both experiments. It was observed that the cells treated both with 0.04 mg/mL nanoparticle and the laser did not demonstrate a significant decrease in viability compared to the cells treated with only 0.04 mg/mL nanoparticle. On the other hand, for the cells treated with 0.08 mg/mL nanoparticle and the laser, the viability further decreased by 50% reaching a final value of 20%. This effect might be attributed to the increased level of PD inside the MCF-7 cells with increased level of EST/PD/RB-BT concentration which results in the increased level of photothermal effect exerted on the MCF-7 cells.

In addition, although the dark toxicity experiment results revealed that the cell viability increased from day 1 to day 3, the photothermal treatment results (with 0.08 mg/mL) show a promising effect in terms of canceling out the viability increase brought by the estrogen incorporated to the nanoparticle structure.

3.4. Conclusion

The *in vitro* effect of NIR- responsive Est/PD/RB-BT nanoparticles was investigated. The particle cytotoxicity was evaluated for concentrations between 0.01 and 0.08 mg/mL on MCF-7 and BEAS-2B cell lines. The cellular uptake of the particles could not be observed after 3 hours and 6 hours of particle incubation; They could be visualized after 12 hours of incubation with the cells. This was attributed to the negative surface charge and the size of the Est/PD/RB-BT nanoparticles. The estrogen incorporation to the particles increased their uptake by 70%. *In vitro* photothermal effect was evaluated for the concentrations of 0.04 mg/mL and 0.08 mg/mL. The results revealed that the 0.04 mg/mL concentration could not achieve a significant effect, whereas the viability drops down to 20 % upon the incubation with 0.08 mg/mL nanoparticle and the laser irradiation. Therefore, the concentration of 0.08 mg/mL presents a better photothermal effect on MCF-7 cells.

CHAPTER 4: INVESTIGATION OF THE *IN VITRO* PHOTODYNAMIC EFFECT OF NIR-RESPONSIVE NANOSTRUCTURE

4.1. Introduction

4.1.1. Photodynamic Effect and PDT

PDT is a type of phototherapy that requires the presence of three components: oxygen, photosensitizer, and a light source. Upon light irradiation, the photosensitizer generates singlet oxygen which is a form of ROS that can damage the molecules inside the cells. This damage in turn triggers cell death through autophagic, apoptotic, or necrotic pathways (Kucinska et al., 2015). Upon light irradiation, the photosensitizer is transferred to the excited singlet state. It then is transferred to the excited triplet state through the intersystem crossing. Being at the excited triplet state, the PS can generate ROS through two different paths as it is demonstrated in Figure 16. In the Type I mechanism, the PS in the triplet state can transfer electrons to a substrate that results in ROS generation. On the other hand, in the Type II mechanism, the PS in the triplet state transfers its energy to triplet oxygen, ground state molecular oxygen, as the PS returns to its ground state.

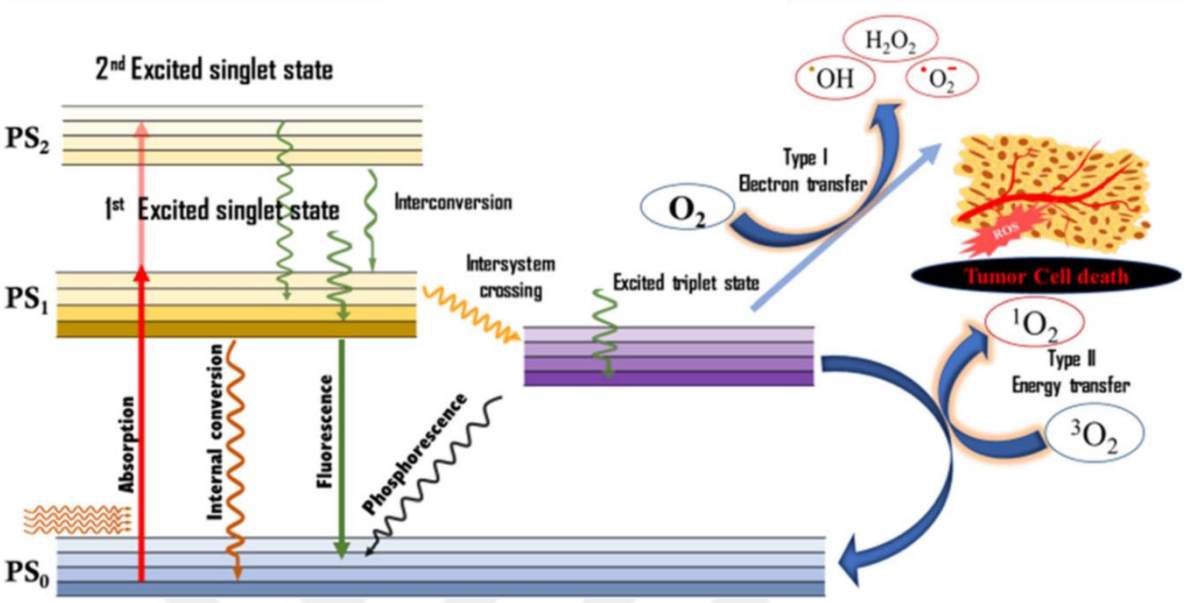

Figure 16 Jablonski diagram that represents the PDT [Modified from: (Baskaran et al., 2018)]

The PS to be used is expected to possess some properties in order to make the PDT more efficient such as high absorption ability and high efficiency in free radical production (Sztandera et al., 2021).

4.1.2. Rose Bengal

Rose Bengal is an FDA-approved dianionic fluorescent dye that is used in the treatment of skin conditions and various cancer types (Sztandera et al., 2021). It has a high singlet oxygen quantum yield Φ_{RB}=0.75 in water (Entradas et al., 2020). The $^1O_2$ generation mechanism for RB is usually through the Type II PDT mechanism (Riley, 1994). Its absorption spectra are given in Figure 17. As it can be seen from Figure 17, RB has a strong absorption near 550 nm.

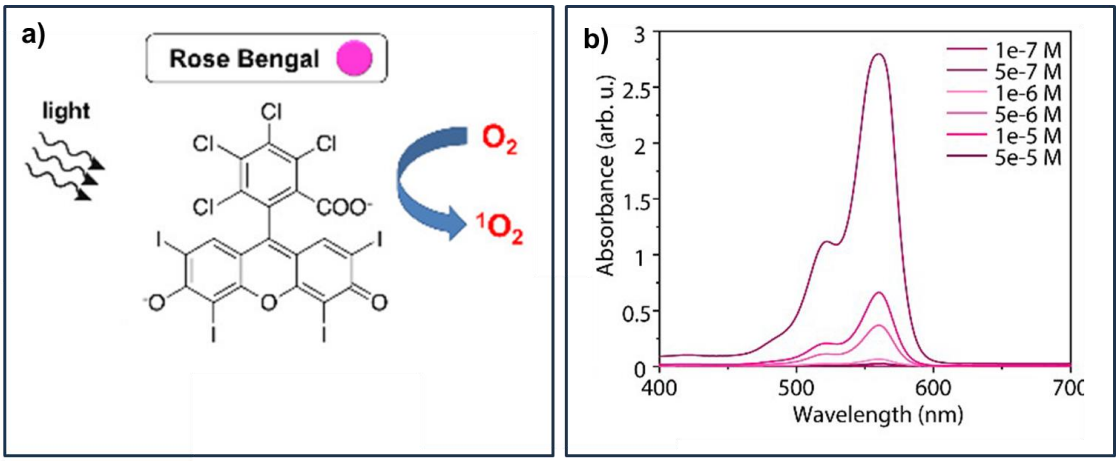

Figure 17 a) The RB molecular structure and representation of $^1O_2$ generation (Sztandera et al., 2021) b) UV absorption spectra of RB (Nsubuga et al., 2021)

4.1.3. Barium Titanate

BT is a metal oxide that is in the form of a perovskite structure. It is a polymorph that can be in the form of rhombohedral, orthorhombic, tetragonal, cubic, or hexagonal depending on the temperature (Figure 18). It demonstrates centrosymmetric properties when it is in the form of cubic or hexagonal structures, whereas when it is in the form of rhombohedral, orthorhombic, and tetragonal, it is a non-centrosymmetric crystal.

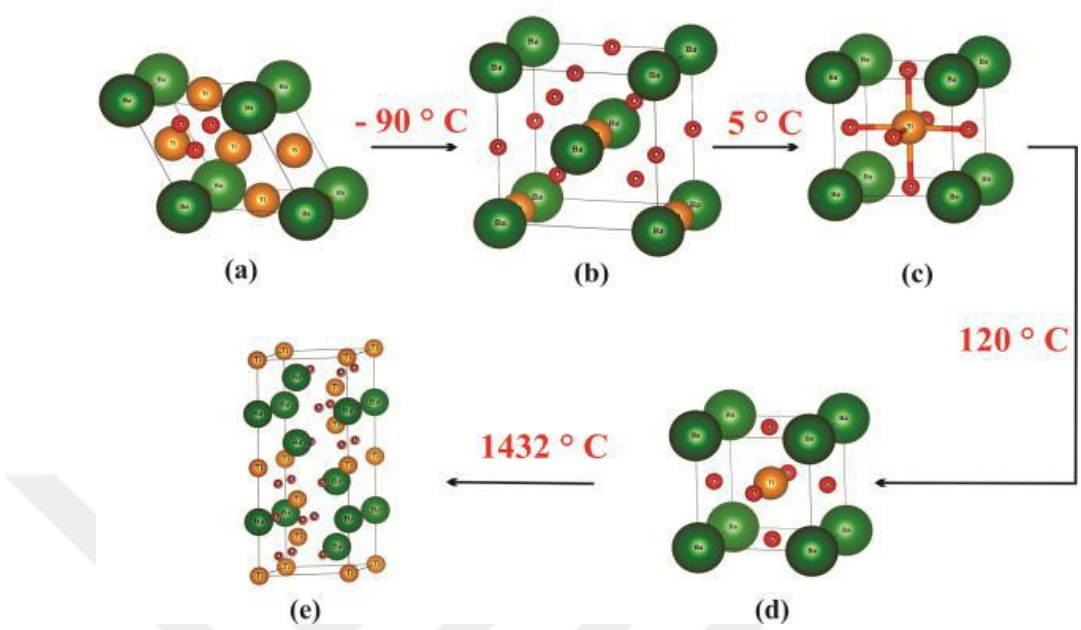

Figure 18 Crystal structure of BT a) Rhombohedral, b) Orthorhombic, c) Tetragonal, d) Cubic, e) Hexagonal (Lacerda et al., 2015)

When it is in any of the 3 forms where it is a non-centrosymmetric crystal, BT does not have an inversion center. Therefore, it can demonstrate properties such as piezoelectricity, and non-linear optical properties.

SHG is a non-linear optical process whereby two photons with the same frequency are absorbed by the material simultaneously and a photon with the doubled frequency is emitted (Ma et al., 2017). However, the simultaneous absorption of two photons with the same frequency has a very low probability unless the light source is a laser, which can produce coherent waves and a high electric field (Karvounis et al., 2020). The second-order nonlinear coefficients displayed by the tetragonal structure of BT enable an efficient SHG process (Ma et al., 2017).

4.1.4. Aim of the study

To generate the photodynamic effect to trigger ROS production within the cell, the RB-BT

complex was integrated inside the PD. The effect is aimed to be triggered by the excitation of particles that are incubated with cells by first irradiating them with a 808 nm laser to release the RB-BT from PD, and then by a pulsed laser with a spectral width of 940 - 1060 nm (central wavelength, $\lambda \cong 1030$ nm). Upon irradiation, the BT is expected to go through frequency doubling and excite the RB to drive cell death through ROS generation.

4.2. Materials and Methods

4.2.1. Materials

DMEM (Pan Biotech), FBS (South America, Pan Biotech), L-glutamine (Pan Biotech), Penicillin-Streptomycin (100X) (Pan Biotech), Trypsin-EDTA (Pan Biotech), Phosphate Buffered Saline (1X) (Pan Biotech), WST-8 Kit (Sigma Aldrich), Hoechst 33342 (Invitrogen).

4.2.2. Methods

4.2.1. Investigation of *In Vitro* Photodynamic Effect of RB-BT Nanoparticles

The photodynamic effect of the Est/PD/RB-BT particles on MCF-7 cells was evaluated upon irradiation with a pulsed femtosecond (fs) laser (central wavelength, $\lambda \cong 1030$ nm; 35 fs; 50 Mhz). The cells were seeded in two different 96-well plates at a density of 1×10^4 cells/well for 24 hours. Then, the medium was replaced with fresh medium containing RB-BT nanoparticles (0.3 mg/mL). Following 24 hours of incubation, the medium containing RB-BT nanoparticles was replaced with a fresh medium. Then, the cells in one of the plates were irradiated with fs laser at a power of 290 mW for 20 minutes or 60 minutes. Upon the completion of laser irradiation, the plates were incubated for 24 hours, and the WST-8 assay was conducted to evaluate the decrease in cell viability caused by the photodynamic effect.

4.2.2. Investigation of *In Vitro* Photodynamic Effect of Est/PD/RB-BT Nanoparticles

The photodynamic effect of the Est/PD/RB-BT particles on MCF-7 cells was evaluated upon the consecutive irradiation by 808 nm CW laser and the same fs laser, respectively. The cells were seeded in two different 96-well plates at a density of 1 x 10^4 cells/well for 24 hours. Then, the medium was replaced with fresh medium containing Est/PD/RB-BT nanoparticles (0.04 mg/mL). Following 20 hours of incubation, the cells in one of the plates were irradiated with CW laser (1.5 W) for 30 mins, and then with fs laser (290 mW) for 30 minutes, whereas the other plate was not irradiated. The plates were incubated for 24 hours after the laser irradiation, and the WST-8 assay was conducted to evaluate the decrease in cell viability caused by the photodynamic effect.

4.3. Results and Discussion

4.3.1. Investigation of *In Vitro* Photodynamic Effect of RB-BT Nanoparticles

The results regarding the *in vitro* photodynamic effect created by RB-BT nanostructures are presented in Figure 19.

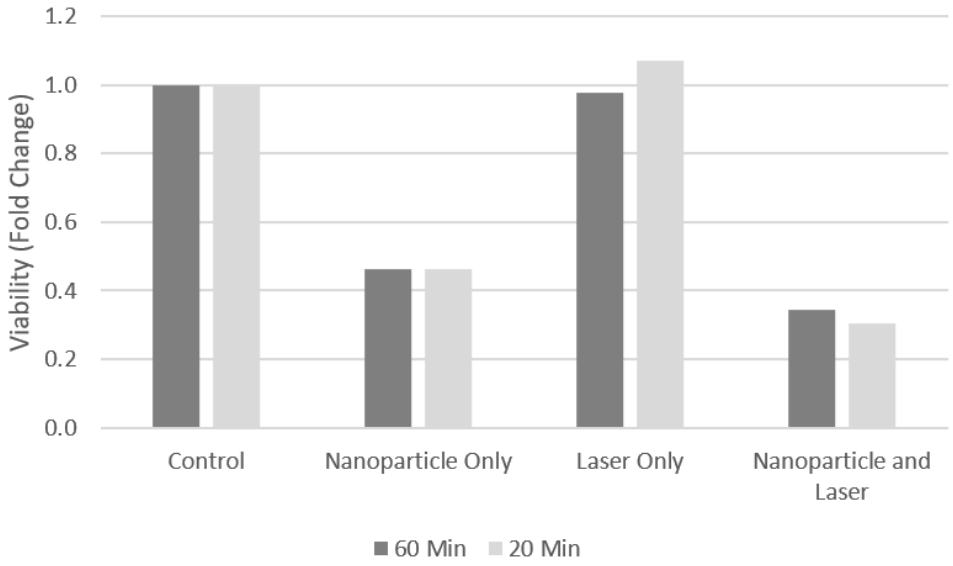

Figure 19 The change in MCF-7 cell viability upon treatment with RB-BT nanostructures and fs laser treatment

The preliminary studies demonstrated that the treatment with only nanoparticles showed about a 50% decrease in viability. The fs laser irradiation itself did not affect the cell viability. The laser irradiation of the nanoparticle-treated group on the other hand demonstrated approximately a further 15% decrease in viability. Therefore, the preliminary studies point out that the BT was successfully irradiated by fs laser, SHG was triggered, and RB could achieve the cell death.

4.3.2. Investigation of *In Vitro* Photodynamic Effect of Est/PD/RB-BT Nanoparticles

Following the experiments with RB-BT particles, the cell death resulting from the interaction of Est/PD/RB-BT nanoparticles with laser was investigated. For this purpose, 808 nm CW laser irradiation was preceded by fs laser irradiation in order to release the RB-BT particles from the PD structure. The results were shown in Figure 20.

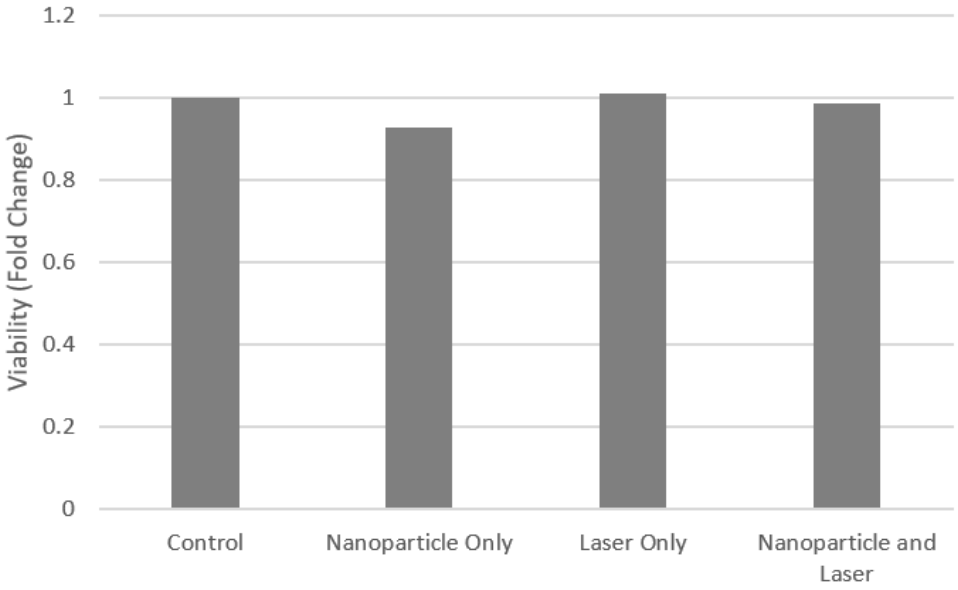

Figure 20 The change in MCF-7 cell viability upon treatment with Est/PD/RB-BT nanostructures and combined laser irradiation.

The "Nanoparticle Only" group showed an insignificant decrease in viability compared to the control group. The "Laser Only" group, which is treated both with CW and fs laser did not seem to be affected by the laser irradiation. However, the experimental group "Nanoparticle and Laser" also did not demonstrate a viability decrease. As depicted in Figure 19, high RB-BT concentration could trigger further cell death upon light irradiation. There are ongoing studies to observe the photodynamic effect of Est/PD/RB-BT on cells by using different parameters.

4.4. Conclusion

The photodynamic effect of RB-BT and Est/PD/RB-BT nanoparticles were evaluated *in vitro*. The RB-BT nanostructures demonstrated a further decrease in viability upon light irradiation, compared to the control group treated with only nanoparticles. However, the photodynamic effect triggered by the Est/PD/RB-BT particles could not be observed on

MCF-7 cells. There are ongoing studies to observe the photodynamic effect of Est/PD/RB-BT particles.

CHAPTER 5: CONCLUSION

In this work, the *in vitro* effect of a multifunctional DDS was investigated. The novel DDS was planned to be implanted at the site of the disease just after the surgery and target the complete removal of remaining cancerous cells and activate the immune response against the local recurrence and metastasis. It constitutes two main subunits: (i) the HER2 and IGF-IR incorporated PLGA implantable patch, and (ii) the NIR-responsive nanostructure Est/PD/RB-BT that was aimed at presenting site-specific treatment for ER+ breast cancer via combined photothermal and photodynamic therapy. In Chapter 2, the release performance from the patches, their toxicity, their uptake by BDCM cells, and their success in the activation of the immune system were evaluated. The uncoated patches were found to be biocompatible, whereas poly (DMAEMA-co-EGDMA) coating introduced toxicity to the patches. Only the IGF-IR could be detected on BDCM cells, and this result is mostly attributed to the higher levels of IGF-IR release from the patches compared to that of HER2. The secretion of TNF-α and IL-2 cytokines demonstrated that the T cells were successfully activated by HER2, and IGF-IR released by the patches. In Chapter 3, the Est/PD/RB-BT particle toxicity, uptake, and its photothermal effect were investigated. It was concluded that the particles cause increased viability at day 3 compared to day 1 due to the estrogen that they include within the structure. The uptake ratio increased by the integration of estrogen to the nanostructure. For the photothermal treatment of the cells, the nanoparticles at a concentration of 0.08 mg/mL showed a sharp decrease in viability, however these concentrations were found to be toxic to healthy cells. The decreased concentration, on the other hand, did not lead to hyperthermia-induced cell death. There are ongoing studies for the observation of optimized concentration. In Chapter 4, the photodynamic effect induced by RB-BT particles and Est/PD/RB-BT particles was investigated. Once irradiated by laser, RB-BT structures lead to a decrease in viability compared to the control groups. With the

Est/PD/RB-BT nanoparticles, however, the viability decrease of MCF-7 cells was not observed. Although the NIR-responsive nanostructure and laser irradiation experiments need to be further studied to achieve better results, it is concluded that this novel multifunctional DDS stands as a promising alternative as it provides a good *in vitro* performance for the treatment of breast cancer.

BIBLIOGRAPHY

Agrawal H, Thacker Nipa, & Misra Ambikanandan. (2011). Parenteral Delivery of Peptides and Proteins. In Misra Ambikanandan (Ed.), Challenges in Delivery of Therapeutic Genomics and Proteomics (pp. 531–622).

Akpan, U. M., Pellegrini, M., Obayemi, J. D., Ezenwafor, T., Browl, D., Ani, C. J., Yiporo, D., Salifu, A., Dozie-Nwachukwu, S., Odusanya, S., Freeman, J., & Soboyejo, W. O. (2020). Prodigiosin-loaded electrospun nanofibers scaffold for localized treatment of triple negative breast cancer. Materials Science and Engineering C, 114. https://doi.org/10.1016/j.msec.2020.110976

Alamdari, S. G., Amini, M., Jalilzadeh, N., Baradaran, B., Mohammadzadeh, R., Mokhtarzadeh, A., & Oroojalian, F. (2022). Recent advances in nanoparticle-based photothermal therapy for breast cancer. In Journal of Controlled Release (Vol. 349, pp. 269–303). Elsevier B.V. https://doi.org/10.1016/j.jconrel.2022.06.050

An, L., Zheng, L., Xu, C., Zhao, Z., Gao, F., Wang, W., Ou, C., & Dong, X. (2023). Organic Charge-Transfer Complexes for Near-Infrared-Triggered Photothermal Materials. Small Structures, 4(1), 2200220. https://doi.org/10.1002/sstr.202200220

Baskaran, R., Lee, J., & Yang, S. G. (2018). Clinical development of photodynamic agents and therapeutic applications. In Biomaterials Research (Vol. 22). BioMed Central Ltd. https://doi.org/10.1186/s40824-018-0140-z

Behzadi, S., Serpooshan, V., Tao, W., Hamaly, M. A., Alkawareek, M. Y., Dreaden, E. C., Brown, D., Alkilany, A. M., Farokhzad, O. C., & Mahmoudi, M. (2017). Cellular uptake of nanoparticles: Journey inside the cell. In Chemical Society Reviews (Vol. 46, Issue 14, pp. 4218–4244). Royal Society of Chemistry. https://doi.org/10.1039/c6cs00636a

Boucher, J., Tseng, Y. H., & Kahn, C. R. (2010). Insulin and insulin-like growth factor-1 receptors act as ligand-specific amplitude modulators of a common pathway regulating gene transcription. Journal of Biological Chemistry, 285(22), 17235–17245. https://doi.org/10.1074/jbc.M110.118620

WHO. (2021, March 26). Breast cancer. https://www.who.int/news-room/fact-sheets/detail/breast-cancer

Buchner, M., García Calavia, P., Muhr, V., Kröninger, A., Baeumner, A. J., Hirsch, T., Russell, D. A., & Marín, M. J. (2019). Photosensitiser functionalised luminescent upconverting nanoparticles for efficient photodynamic therapy of breast cancer cells. Photochemical and Photobiological Sciences, 18(1), 98–109. https://doi.org/10.1039/c8pp00354h

Cai, S., Yan, J., Xiong, H., Wu, Q., Xing, H., Liu, Y., Liu, S., & Liu, Z. (2020). Aptamer-functionalized molybdenum disulfide nanosheets for tumor cell targeting and lysosomal acidic environment/NIR laser responsive drug delivery to realize synergetic chemo-photothermal therapeutic effects. International Journal of Pharmaceutics, 590. https://doi.org/10.1016/j.ijpharm.2020.119948

Caroline, D. S. M., & Rekha, M. R. (2022). Exploring the efficacy of ethylene glycol dimethacrylate crosslinked cationised pullulan for gene delivery in cancer cells. Journal of Drug Delivery Science and Technology, 68. https://doi.org/10.1016/j.jddst.2021.103067

Chew, S. A., & Danti, S. (2017). Biomaterial-Based Implantable Devices for Cancer Therapy. In Advanced Healthcare Materials (Vol. 6, Issue 2). Wiley-VCH Verlag. https://doi.org/10.1002/adhm.201600766

Cho, H. S., & Leahy, D. J. (2002). Structure of the extracellular region of HER3 reveals an interdomain tether. Science, 297(5585), 1330–1333. https://doi.org/10.1126/science.1074611

Ward C, Thomas P.J. Garrett, Mei Lou, Neil M. Mckern, Timothy E. Adams, Thomas C. Elleman, Peter A. Hoyne, Maurice J. Frenkel, Leah J. Cosgrove, & George O. Lovrecz. (2000). The Structure of the Type 1 Insulin-Like Growth Factor Receptor. Landes Bioscience. https://www.ncbi.nlm.nih.gov/books/NBK6216/

Costa, B., Amorim, I., Gärtner, F., & Vale, N. (2020). Understanding Breast cancer: from conventional therapies to repurposed drugs. In European Journal of Pharmaceutical Sciences (Vol. 151). Elsevier B.V. https://doi.org/10.1016/j.ejps.2020.105401

Dong, Z., Gong, H., Gao, M., Zhu, W., Sun, X., Feng, L., Fu, T., Li, Y., & Liu, Z. (2016a). Polydopamine nanoparticles as a versatile molecular loading platform to enable imaging-

guided cancer combination therapy. Theranostics, 6(7), 1031–1042. https://doi.org/10.7150/thno.14431

Dong, Z., Gong, H., Gao, M., Zhu, W., Sun, X., Feng, L., Fu, T., Li, Y., & Liu, Z. (2016b). Polydopamine nanoparticles as a versatile molecular loading platform to enable imaging-guided cancer combination therapy. Theranostics, 6(7), 1031–1042. https://doi.org/10.7150/thno.14431

Entradas, T., Waldron, S., & Volk, M. (2020). The detection sensitivity of commonly used singlet oxygen probes in aqueous environments. Journal of Photochemistry and Photobiology B: Biology, 204. https://doi.org/10.1016/j.jphotobiol.2020.111787

Fan, S., Lin, W., Huang, Y., Xia, J., Xu, J. F., Zhang, J., & Pi, J. (2022). Advances and Potentials of Polydopamine Nanosystem in Photothermal-Based Antibacterial Infection Therapies. In Frontiers in Pharmacology (Vol. 13). Frontiers Media S.A. https://doi.org/10.3389/fphar.2022.829712

Gleason, K. K. (2021). Controlled Release Utilizing Initiated Chemical Vapor Deposited (iCVD) of Polymeric Nanolayers. In Frontiers in Bioengineering and Biotechnology (Vol. 9). Frontiers Media S.A. https://doi.org/10.3389/fbioe.2021.632753

Grobmyer, S. R., Zhou, G., Gutwein, L. G., Iwakuma, N., Sharma, P., & Hochwald, S. N. (2012). Nanoparticle delivery for metastatic breast cancer. In Nanomedicine: Nanotechnology, Biology, and Medicine (Vol. 8, Issue SUPPL. 1). https://doi.org/10.1016/j.nano.2012.05.011

Guermonprez, P., Valladeau, J., Zitvogel, L., Théry, C., & Amigorena, S. (2002a). Antigen presentation and T cell stimulation by dendritic cells. In Annual Review of Immunology (Vol. 20, pp. 621–667). https://doi.org/10.1146/annurev.immunol.20.100301.064828

Guermonprez, P., Valladeau, J., Zitvogel, L., Théry, C., & Amigorena, S. (2002b). Antigen presentation and T cell stimulation by dendritic cells. In Annual Review of Immunology (Vol. 20, pp. 621–667). https://doi.org/10.1146/annurev.immunol.20.100301.064828

Guo, S., Song, Z., Ji, D. K., Reina, G., Fauny, J. D., Nishina, Y., Ménard-Moyon, C., & Bianco, A. (2022). Combined Photothermal and Photodynamic Therapy for Cancer

Treatment Using a Multifunctional Graphene Oxide. Pharmaceutics, 14(7). https://doi.org/10.3390/pharmaceutics14071365

Gutierrez, C., & Schiff, R. (2011). HER 2: Biology, Detection, and Clinical Implications. https://doi.org/10.1043/2010-0454-RAR.1

Higbee-Dempsey, E., Amirshaghaghi, A., Case, M. J., Miller, J., Busch, T. M., & Tsourkas, A. (2019). Indocyanine Green–Coated Gold Nanoclusters for Photoacoustic Imaging and Photothermal Therapy. Advanced Therapeutics, 2(9). https://doi.org/10.1002/adtp.201900088

Hope, A., Wade, S. J., Aghmesheh, M., & Vine, K. L. (2022). Localized delivery of immunotherapy via implantable scaffolds for breast cancer treatment. In Journal of Controlled Release (Vol. 341, pp. 399–413). Elsevier B.V. https://doi.org/10.1016/j.jconrel.2021.11.043

Hussain, T., Ramakrishna, S., & Abid, S. (2022). Nanofibrous drug delivery systems for breast cancer: A review. In Nanotechnology (Vol. 33, Issue 10). IOP Publishing Ltd. https://doi.org/10.1088/1361-6528/ac385c

Janeway CA Jr, Travers P, & Walport M. (2001). Principles of innate and adaptive immunity. In Immunobiology: The Immune System in Health and Disease. 5th edition. (5th ed.). Garland Science.

Jaque, D., Martínez Maestro, L., Del Rosal, B., Haro-Gonzalez, P., Benayas, A., Plaza, J. L., Martín Rodríguez, E., & García Solé, J. (2014). Nanoparticles for photothermal therapies. Nanoscale, 6(16), 9494–9530. https://doi.org/10.1039/c4nr00708e

Jayakumar, R., Prabaharan, M., Nair, S. V., & Tamura, H. (2010). Novel chitin and chitosan nanofibers in biomedical applications. In Biotechnology Advances (Vol. 28, Issue 1, pp. 142–150). https://doi.org/10.1016/j.biotechadv.2009.11.001

Jones, R. A., Campbell, C. I., Gunther, E. J., Chodosh, L. A., Petrik, J. J., Khokha, R., & Moorehead, R. A. (2007). Transgenic overexpression of IGF-IR disrupts mammary ductal morphogenesis and induces tumor formation. Oncogene, 26(11), 1636–1644. https://doi.org/10.1038/sj.onc.1209955

Karvounis, A., Timpu, F., Vogler-Neuling, V. V., Savo, R., & Grange, R. (2020). Barium Titanate Nanostructures and Thin Films for Photonics. In Advanced Optical Materials (Vol. 8, Issue 24). Wiley-VCH Verlag. https://doi.org/10.1002/adom.202001249

Kefayat, A., & Vaezifar, S. (2019). Biodegradable PLGA implants containing doxorubicin-loaded chitosan nanoparticles for treatment of breast tumor-bearing mice. International Journal of Biological Macromolecules, 136, 48–56. https://doi.org/10.1016/j.ijbiomac.2019.06.055

Kharbanda, S., Salter, R. D., Dong, X., Tuma-Warrino, R. J., & Steinman, R. A. (2002). BDCM: a novel B-cell line with genetic and functional similarity to dendritic cells.

Kucinska, M., Skupin-Mrugalska, P., Szczolko, W., Sobotta, L., Sciepura, M., Tykarska, E., Wierzchowski, M., Teubert, A., Fedoruk-Wyszomirska, A., Wyszko, E., Gdaniec, M., Kaczmarek, M., Goslinski, T., Mielcarek, J., & Murias, M. (2015). Phthalocyanine derivatives possessing 2-(morpholin-4-yl)ethoxy groups as potential agents for photodynamic therapy. Journal of Medicinal Chemistry, 58(5), 2240–2255. https://doi.org/10.1021/acs.jmedchem.5b00052

Lacerda, L. H. da S., Ribeiro, R. A. P., Andrade, A. M. de, & Lazaro, S. R. de. (2015). Zn-doped BaTiO3 Materials: A DFT Investigation for Optoelectronic and Ferroelectric Properties Improvement. Revista Processos Químicos, 9(18), 274–280. https://doi.org/10.19142/rpq.v9i18.323

Lamberti, M. J., Rumie Vittar, N. B., & Rivarola, V. A. (2014). Breast cancer as photodynamic therapy target: Enhanced therapeutic efficiency by overview of tumor complexity. World Journal of Clinical Oncology, 5(5), 901–907. https://doi.org/10.5306/wjco.v5.i5.901

Lee, H. L., Jang, J. W., Lee, S. W., Yoo, S. H., Kwon, J. H., Nam, S. W., Bae, S. H., Choi, J. Y., Han, N. I., & Yoon, S. K. (2019). Inflammatory cytokines and change of Th1/Th2 balance as prognostic indicators for hepatocellular carcinoma in patients treated with transarterial chemoembolization. Scientific Reports, 9(1). https://doi.org/10.1038/s41598-019-40078-8

Lee, J. J., Yazan, L. S., & Abdullah, C. A. C. (2017). A review on current nanomaterials and their drug conjugate for targeted breast cancer treatment. In International Journal of

Nanomedicine (Vol. 12, pp. 2373–2384). Dove Medical Press Ltd. https://doi.org/10.2147/IJN.S127329

Li, J., Zhang, W., Ji, W., Wang, J., Wang, N., Wu, W., Wu, Q., Hou, X., Hu, W., & Li, L. (2021). Near infrared photothermal conversion materials: mechanism, preparation, and photothermal cancer therapy applications. In Journal of Materials Chemistry B (Vol. 9, Issue 38, pp. 7909–7926). Royal Society of Chemistry. https://doi.org/10.1039/d1tb01310f

Li, M., Sun, X., Zhang, N., Wang, W., Yang, Y., Jia, H., & Liu, W. (2018). NIR-Activated Polydopamine-Coated Carrier-Free "Nanobomb" for In Situ On-Demand Drug Release. Advanced Science, 5(7). https://doi.org/10.1002/advs.201800155

Li, X., He, Y., Hou, J., Yang, G., & Zhou, S. (2020). A Time-Programmed Release of Dual Drugs from an Implantable Trilayer Structured Fiber Device for Synergistic Treatment of Breast Cancer. Small, 16(9). https://doi.org/10.1002/smll.201902262

Li, X., Xu, F., He, Y., Li, Y., Hou, J., Yang, G., & Zhou, S. (2020). A Hierarchical Structured Ultrafine Fiber Device for Preventing Postoperative Recurrence and Metastasis of Breast Cancer. Advanced Functional Materials, 30(45). https://doi.org/10.1002/adfm.202004851

Liew F. Y. (2002). TH1 and TH2 cells: a historical perspective. Nature Reviews, 2, 55–59.

Lowell A. (2020, July 29). Immunology Overview: How Does Our Immune System Protect Us?

Luckheeram, R. V., Zhou, R., Verma, A. D., & Xia, B. (2012). CD4 +T cells: Differentiation and functions. In Clinical and Developmental Immunology (Vol. 2012). https://doi.org/10.1155/2012/925135

Lykkesfeldt, A. E., & Sqrensen, E. K. (1992). Effect of estrogen and antiestrogens on cell proliferation and synthesis of secreted proteins in the human breast cancer cell line MCF-7 and a tamoxifen resistant variant subline, AL-1. Acta Oncologica, 31(2), 131–138. https://doi.org/10.3109/02841869209088892

Ma, C., Yan, J., Wei, Y., Liu, P., & Yang, G. (2017). Enhanced second harmonic generation in individual barium titanate nanoparticles driven by Mie resonances. Journal of Materials Chemistry C, 5(19), 4810–4819. https://doi.org/10.1039/c7tc00650k

Mayrovitz, H. N. (2022). Breast Cancer. Exon.

Mfouo-Tynga, I., Houreld, N. N., & Abrahamse, H. (2018). Evaluation of cell damage induced by irradiated Zinc-Phthalocyanine-gold dendrimeric nanoparticles in a breast cancer cell line. Biomedical Journal, 41(4), 254–264. https://doi.org/10.1016/j.bj.2018.05.002

Moorthi, C., Manavalan, R., & Kathiresan, K. (2011). Nanotherapeutics to Overcome Conventional Cancer Chemotherapy Limitations. In J Pharm Pharmaceut Sci (www.cspsCanada.org) (Vol. 14, Issue 1). www.cspsCanada.org

Nsubuga, A., Mandl, G. A., & Capobianco, J. A. (2021). Investigating the reactive oxygen species production of Rose Bengal and Merocyanine 540-loaded radioluminescent nanoparticles. Nanoscale Advances, 3(5), 1375–1381. https://doi.org/10.1039/d0na00964d

Park, M., Kim, D., Ko, S., Kim, A., Mo, K., & Yoon, H. (2022). Breast Cancer Metastasis: Mechanisms and Therapeutic Implications. In International Journal of Molecular Sciences (Vol. 23, Issue 12). MDPI. https://doi.org/10.3390/ijms23126806

PESTRONK, A., & LOPATE, G. (2005). Chapter 97 - Polyneuropathies and Antibodies to Nerve Components. In P. J. Dyck & P. K. Thomas (Eds.), Peripheral Neuropathy (Fourth Edition) (Fourth Edition, pp. 2177–2196). W.B. Saunders. https://doi.org/https://doi.org/10.1016/B978-0-7216-9491-7.50100-9

Pial, M. M. H., Tomitaka, A., Pala, N., & Roy, U. (2022). Implantable Devices for the Treatment of Breast Cancer. Journal of Nanotheranostics, 3(1), 19–38. https://doi.org/10.3390/jnt3010003

Ramasethu, J. (2004). Chapter 18 - Hemolytic Disease of the Newborn. In C. D. Hillyer, R. G. Strauss, & N. L. C. Luban (Eds.), Handbook of Pediatric Transfusion Medicine (pp. 191–208). Academic Press. https://doi.org/https://doi.org/10.1016/B978-012348776-6/50021-2

Raza, A., Rasheed, T., Nabeel, F., Hayat, U., Bilal, M., & Iqbal, H. M. N. (2019). Endogenous and exogenous stimuli-responsive drug delivery systems for programmed site-specific release. In Molecules (Vol. 24, Issue 6). MDPI AG. https://doi.org/10.3390/molecules24061117

Reichl, F. X., Seiss, M., Buters, J., Behrendt, H., Hickel, R., & Durner, J. (2010). Expression of CYP450-2E1 and formation of 2,3-epoxymethacrylic acid (2,3-EMA) in human oral cells exposed to dental materials. Dental Materials, 26(12), 1151–1156. https://doi.org/10.1016/j.dental.2010.08.005

Riley, P. A. (1994). Free radicals in biology : oxidative stress and the effects of ionizing radiation. In INT. J. RADIAT. BIOL (Vol. 65, Issue 1).

Sapra Sharma, P., Sharma, R., & Tyagi, T. (2009). Receptor Tryosine Kinase Inhibitors as Potent Weapons in War Against Cancers. In Current Pharmaceutical Design (Vol. 15). http://www.pdb.org

Sedghi, R., Shaabani, A., Mohammadi, Z., Samadi, F. Y., & Isaei, E. (2017). Biocompatible electrospinning chitosan nanofibers: A novel delivery system with superior local cancer therapy. Carbohydrate Polymers, 159, 1–10. https://doi.org/10.1016/j.carbpol.2016.12.011

Shapero, K., Fenaroli, F., Lynch, I., Cottell, D. C., Salvati, A., & Dawson, K. A. (2011). Time and space resolved uptake study of silica nanoparticles by human cells. Molecular BioSystems, 7(2), 371–378. https://doi.org/10.1039/c0mb00109k

Shi, X., Cheng, Y., Wang, J., Chen, H., Wang, X., Li, X., Tan, W., & Tan, Z. (2020). 3D printed intelligent scaffold prevents recurrence and distal metastasis of breast cancer. Theranostics, 10(23), 10652–10664. https://doi.org/10.7150/thno.47933

Shibu, E. S., Hamada, M., Murase, N., & Biju, V. (2013). Nanomaterials formulations for photothermal and photodynamic therapy of cancer. In Journal of Photochemistry and Photobiology C: Photochemistry Reviews (Vol. 15, Issue 1, pp. 53–72). https://doi.org/10.1016/j.jphotochemrev.2012.09.004

Soukasene, S., Toft, D. J., Moyer, T. J., Lu, H., Lee, H. K., Standley, S. M., Cryns, V. L., & Stupp, S. I. (2011). Antitumor activity of peptide amphiphile nanofiber-encapsulated camptothecin. ACS Nano, 5(11), 9113–9121. https://doi.org/10.1021/nn203343z

Sudhesh Dev, S., Zainal Abidin, S. A., Farghadani, R., Othman, I., & Naidu, R. (2021). Receptor Tyrosine Kinases and Their Signaling Pathways as Therapeutic Targets of

Curcumin in Cancer. In Frontiers in Pharmacology (Vol. 12). Frontiers Media S.A. https://doi.org/10.3389/fphar.2021.772510

Szeimies, R. M., Morton, C. A., Sidoroff, A., & Braathen, L. R. (2005). Photodynamic therapy for non-melanoma skin cancer. In Acta Dermato-Venereologica (Vol. 85, Issue 6, pp. 483–490). https://doi.org/10.1080/00015550510044136

Sztandera, K., Gorzkiewicz, M., Dias Martins, A. S., Pallante, L., Zizzi, E. A., Miceli, M., Bątal, M., Reis, C. P., Deriu, M. A., & Klajnert-Maculewicz, B. (2021). Noncovalent Interactions with PAMAM and PPI Dendrimers Promote the Cellular Uptake and Photodynamic Activity of Rose Bengal: The Role of the Dendrimer Structure. Journal of Medicinal Chemistry, 64(21), 15758–15771. https://doi.org/10.1021/acs.jmedchem.1c01080

Wong, B. S. T., Hsu, B. A. L., & Liao, M. D. W. (n.d.). Phototherapy in Psoriasis: A Review of Mechanisms of Action.

Zhou, S., Li, D., Lee, C., & Xie, J. (2020). Nanoparticle Phototherapy in the Era of Cancer Immunotherapy. In Trends in Chemistry (Vol. 2, Issue 12, pp. 1082–1095). Cell Press. https://doi.org/10.1016/j.trechm.2020.09.008